Supporting information for

From metallic gold to $[Au(NHC)_2]^+$ complexes: An easy, one-pot method

Leticia Lozada-Rodríguez,[a] José B. Pelayo-Vázquez,[b] Irma I. Rangel-Salas,[a] José G. Alvarado-Rodríguez,[c] A. Aarón Peregrina-Lucano,[d] Armando Pérez-Centeno,[e] Fernando A. López-Dellamary-Toral,[f] Sara A. Cortes-Llamas[a]*

[a]Departamento de Química, [d]Departamento de Farmacobiología, [e]Departamento de Física; Centro Universitario de Ciencias Exactas e Ingenierías, Universidad de Guadalajara, Blvd. Marcelino García Barragán #1421, esq. Olímpica, C.P. 44430 Guadalajara, Jalisco, México.

[b]Departamento de Ciencias Básicas, Aplicadas e Ingenierías Centro Universitario de Tonalá, Universidad de Guadalajara, Av. Nuevo Periférico No. 555, Ejido San José Tatepozco C.P. 45425, Tonalá Jalisco, México.

[c]Universidad Autónoma del Estado de Hidalgo, Unidad Universitaria, km 4.5 Carretera Pachuca-Tulancingo, C.P. 42184 Mineral de la Reforma, Hidalgo, México.

[f]Departamento de Madera, Celulosa y Papel, Centro Universitario de Ciencias Exactas e Ingenierías, Universidad de Guadalajara, km 15.5 de la Carretera Guadalajara-Nogales, C.P. 45220 Zapopan, Jalisco, México.

sara.cortes@cucei.udg.mx

Contents

Figures

1. General information

All reactions were carried under air. Technical grade solvents were used. All reagents were obtained commercially and utilized as received without further purification. Starting materials for **1c**[1,2] and **1f**[3] were synthesized according to literature. ^{1}H and ^{13}C NMR spectra were recorded on a JEOL ECA 600 MHz spectrometer. Chemical shifts are expressed in parts per million and referenced to residual solvent peaks. IR spectra were recorded with a Thermo Scientific Nicolet iS5 spectrophotometer equipped with iD5 ATR accessory. Melting points were determined on a Mel-Temp apparatus. High resolution mass spectra were obtained by LC/MSD TOF with APCI as ionization source in an Agilent G1969A. ESI-MS spectra were recorded on a 6410B triple quadrupole LC/MS from Agilent Technologies. Raman measurements were performed with a 473 nm solid state laser, whereas the fluorescence spectra were acquired at 360 nm excitation line by using a 1000 W Xe-lamp coupled with a Sciencetech monochromator model 9030; in both optical spectroscopies, the signal was collected to Acton spectrometer model SpectraPro 2750, and the intensity was detected with a Hamamatsu photomultiplier tube model R928. The structural characterization was carried out at room temperature. Single crystal X-ray diffraction data of **2a**, **2c**, **2e**, **2f**, **2h** and **2i**, were collected at room temperature on an Oxford Diffraction Gemini CCD diffractometer with either graphite-monochromated Mo-Kα (λ = 0.71073 Å) or Cu-Kα radiation (λ = 1.54184). Data were integrated, scaled, sorted, and averaged using the CrysAlis software package. By using Olex2,[4] the structures were solved with the ShelXT structure solution program using Direct Methods and refined with the ShelXL,[5] refinement package using Least Squares minimization. All non-hydrogen atoms were refined anisotropically. The positions of the hydrogen atoms were kept fixed with a common isotropic displacement parameter. **2a** displayed three molecules in the asymmetric unit; two of these molecules are related by a two-fold axis containing gold atoms. The vector C-Au-C present in **2e** also lies on a two-fold axis. **2f** crystallized as an acetonitrile solvate and displayed just the half of the complex; both complex cation and anion are also related by a binary axis. Complexes **2a**, **2c**, **2h**, and **2i** displayed positional disorder. The disorder was treated with rigid bond restraints by using instructions such as SAME, SIMU, and RIGU. (reference: For a detailed description of the restraints, see Müller, Peter. "Disorder" Crystal Structure Refinement. A Crystallographer's Guide to SHELXL. Edited by P. Müller. New York: Oxford University Press, 2006. 56-96). CCDC 1522834 (**2a**), 522833 (**2c**), 1522836 (**2e**), 1522832 (**2f**·MeCN), 1522835 (**2h**), and 1522837 (**2i**) contains the supplementary crystallographic data. These data can be obtained free of charge via http://www.ccdc.cam.ac.uk/conts/retrieving.html, or from the Cambridge Crystallographic Data Centre, 12 Union Road, Cambridge CB2 1EZ, UK; fax: (+44) 1223-336-033; or e-mail: deposit@ccdc.cam.ac.uk.

Synthesis of complexes were carried out in an Ace pressure tube (bushing type, front seal, volume approx. 38 mL, L × O.D. 20.3 cm × 25.4 mm).

2. Synthesis of ligands

Ligands were synthesized by means of Cl^- or Br^- replacement by the corresponding non-coordinating anion (BPh_4^-, BF_4^-, PF_6^-) in water, as it is shown below for **1c**, **1f**, **1i**. **1h** was prepared in acetone according to cited procedure.[6] Structural characterization of **1a**,[7] **1b**,[2] **1d**,[8] **1e**,[9] **1g**,[10] and **1h**[6] was consistent with that reported in literature.

2.1 General procedure for ligands 1c, 1f, 1i.

To a stirred aqueous imidazolium salt solution was added sodium tetraphenylborate (1 equiv.) dissolved in water. The mixture was stirred for 20 min at room temperature. The white precipitate was filtered and dried *in vacuum* to afford the desired product.

2.1.1 HIMes·BPh_4 (1c)

1,3-dimesityl-1*H*-imidazol-3-ium chloride[1,2] (2.00 g, 5.86 mmol) suspended in water (400 mL), sodium tetraphenylborate (2.01 g, 5.86 mmol) dissolved in water (40 mL). Yield 94 %. **mp** 206-208 °C. **FT-IR** υ_{max} 3119 (w), 3096 (w), 3048 (w), 1579 (w), 1535 (m), 1476 (m), 1425 (m), 1379 (w), 1245 (m), 1217 (w), 1033 (w), 861 (m), 734 (s), 705 (s), 612 (m) cm^{-1}. **MS**- ESI-TOF-MS(+) (m/z): found 305.2013 $C_{21}H_{25}N_2^+$ requires 305.2012. **^{1}H NMR** (600 MHz, DMSO-d_6) δ ppm 9.64 (s, 1H, NC*H*N), 8.19 - 8.28 (m, 2H, NC*H*C*H*N), 7.20 (s, 12H, Ar*H,* BC_6H_5), 6.93 (t, 8H, BC_6H_5), 6.75 - 6.86 (m, 4H, BC_6H_5), 2.36 (s, 6H, *p*-CH_3) 2.12 (s, 12H, *o*-CH_3). **^{13}C NMR** (151 MHz, DMSO-d_6) δ ppm 163.3 (q, $^1J_{BC}$ = 49.1 Hz, B*C*), 140.6 (Ar*C*), 138.5 (N*C*HN), 135.5 (*o*-BPh_4), 134.3 (Ar*C*), 131.0 (Ar*C*), 129.3 (Ar*C*), 125.3 (t, *m*-BPh_4), 124.8 (N*C*H*C*HN), 121.5 (*p*-BPh_4), 20.6 (*p*-C*C*H_3), 16.9 (*m*-C*C*H_3).

2.1.2 HICy·BPh_4 (1f)

1,3-dicyclohexyl-1*H*-imidazol-3-ium chloride[3] (2.00 g, 7.4 mmol) dissolved in water (100 mL), sodium tetraphenylborate (2.54 g, 7.4 mmol) dissolved in water (40 mL). Yield: 95 %. **mp** 101-103 °C. **FT-IR** υ_{max} 3140 (w), 3051 (w), 2936 (w), 2858 (w), 1579 (w), 1542 (w), 1478 (w), 1450 (w), 1425 (w), 1152 (w), 730 (m), 705 (s), 606 (m) cm^{-1}. **MS**- ESI-TOF-MS(+)

(m/z): found 233.2014 $C_{15}H_{25}N_2^+$ requires 233.2012. **^{1}H NMR** (600 MHz,DMSO-d_6) δ ppm: 9.23 (t, $^4J_{HH}$ = 2.1 Hz, 1H, NC*H*N), 7.89 (d, $^4J_{HH}$ = 2.1 Hz, 2H, NC*H*C*H*N), 7.18 (d, 8H, BC_6H_5), 6.92 (t, 8H, BC_6H_5), 6.81 - 6.75 (m, 4H, BC_6H_5), 4.23 (tt, 2H, NC*H*CH_2), 2.05 (d, 4H, CH_2), 1.83 (d, 4H, CH_2), 1.71 – 1.64 (m, 6H, CH_2), 1.37 (tq, 4H, CH_2), 1.23 - 1.13 (m, 2H, CH_2).**^{13}C NMR** (151 MHz, DMSO-d_6) δ ppm: 163.6 (q, $^1J_{BC}$ = 49.2 Hz, B*C*), 135.5 (*o*-BPh_4), 133.5 (N*C*HN), 125.3 (t, *m*-BPh_4), 121.5 (*p*-BPh_4), 120.8 (N*C*H*C*HN), 58.7 (N*C*HCH_2), 32.4 (*C*H_2), 24.5 (*C*H_2), 24.4 (*C*H_2).

2.1.3 HIEtMe·BPh_4 (1i)

3-ethyl-1-methyl-1*H*-imidazol-3-ium bromide (1.50 g, 7.69 mmol) dissolved in water (80 mL), sodium tetraphenylborate (2.63 g, 7.69 mmol) dissolved in water (40 mL). Yield 95 %. **mp** 161-163 °C. **FT-IR** υ_{max} 3138 (w), 3091 (w), 3050 (w), 2983 (w), 1577 (w), 1565 (w), 1476 (w), 1422 (w), 1163 (m), 1026 (w), 833 (w), 732 (s), 694 (s) cm^{-1}. **MS**- ESI-TOF-MS(+) (m/z): found 111.0917 $C_6H_{11}N_2^+$ requires 111.0917. **^{1}H NMR** (600 MHz, DMSO-d_6) δ ppm 9.05 (s, 1H, NC*H*N), 7.75 (s, 1H, NC*H*CHN), 7.66 (s, 1H, NCHC*H*N), 7.26 - 7.11 (m, 8H, BC_6H_5), 6.93 (t, 8H, BC_6H_5), 6.84 - 6.70 (m, 4H, BC_6H_5), 4.16 (q, $^3J_{HH}$ = 7.6 Hz, 2H, CH_2), 3.81 (s, 3H, NCH_3), 1.39 (t, $^3J_{HH}$ = 7.6 Hz, 3H, CH_2CH_3). **^{13}C NMR** (151 MHz, DMSO-d_6) δ ppm 163.3 (q, $^1J_{BC}$ = 49.2 Hz, B*C*), 136.2 (N*C*HN), 135.5 (*o*-BPh_4), 125.3 (q, *m*-BPh_4), 123.6 (N*C*HCHN), 122.0 (NCH*C*HN), 121.5 (*p*-BPh_4), 44.1 (N*C*H_2), 35.7 (N*C*H_3), 15.1 (CH_2CH_3).

3. Synthesis of complexes (2a-2i)

3.1 General procedure

Powdered gold (25 mg, 0.13 mmol, purity ≥99.9 %, size < 10 µm, from Sigma Aldrich), the corresponding imidazolium salt (0.25 mmol), acetonitrile (15 mL), $CuSO_4·5H_2O$ (500 µL, 0.5 M, 0.25 mmol), and aqueous ammonia solution (10 mL, 28 %) were added to a pressure tube.* The mixture was stirred in an oil bath at 80 °C for 24 hours. Then, it was allowed to cool down to room temperature. The solution was filtered through a nylon membrane (0.20 µm pore diameter) with a syringe. The remaining solid was washed with dichloromethane (3 × 5 mL) and filtered through the same membrane, to ensure completely recovery of the product. The filtered solution was concentrated on a rotavapor to aqueous phase (5-10 mL) and extracted with dichloromethane (3 × 25 mL).

Note: Loss of ammonia results in a low reaction yield. It should be verified that pressure tube seals work correctly to avoid ammonia leaking. In addition, the reaction mixture should be stirred properly, due to the heterogeneous nature of the system.

The organic extracts were combined, dried over anhydrous sodium sulfate and concentrated *in vacuum* to give crude product.

3.1.1 $[Au(IMes)_2]PF_6$ (2a)

HIMes·PF_6 (115 mg, 0.25 mmol). Crude product was washed with tetrahydrofuran (2 mL), decanted, and dried *in vacuum* to obtain the desired product as a white solid. Yield 83 %. **mp** 274 °C (dec.). **FT-IR** υ_{max} 3174 (w), 2919 (w), 1734 (w), 1612 (w), 1490 (m), 1438 (w), 1374 (w), 1235 (m), 1037 (w), 858 (m), 835 (s), 754 (m), 703 (w), 556 (m) cm^{-1}. **MS**- ESI-TOF-MS(+) (m/z): found 805.3535 $C_{42}H_{48}AuN_4^+$ requires 805.3539. **^{1}H NMR** (600 MHz, DMSO-d_6) δ ppm 7.70 (s, 4H, NC*H*C*H*N), 6.99 (s, 8H, Ar*H*), 2.42 (s, 12H, *p*-CH_3), 1.65 ppm (s, 24H, *o*-CH_3). **^{13}C NMR** (151 MHz, DMSO-d_6) δ ppm 184.1 (N*C*N), 138.8 (Ar*C*), 134.1 (two overlapped Ar*C*), 128.7 (Ar*C*), 123.5 (NCH*C*HN), 20.7 (*p*-C*C*H_3), 16.6 (*m*-C*C*H_3). Adequate crystals for X-ray diffraction were grown by slow evaporation from dichloromethane.

3.1.2 $[Au(IMes)_2]BF_4$ (2b)

HIMes·BF_4 (99 mg, 0.25 mmol). Crude product was crystallized by slow evaporation from dichlorometane. Crystals were washed with tetrahydrofuran (1 mL) and dried *in vacuum*. Yield 92 %. **^{1}H NMR** (600 MHz, DMSO-d_6) δ ppm 7.70 (s, 4H, NC*H*C*H*N), 6.99 (s, 8H, Ar*H*), 2.42 (s, 12H, *p*-CH_3), 1.65 ppm (s, 24H, *o*-CH_3). **^{13}C NMR** (151 MHz, DMSO-d_6) δ ppm 184.2 (N*C*N), 139.0 (Ar*C*), 134.2 (two overlapped Ar*C*), 128.9 (Ar*C*), 123.7 (N*C*H*C*HN), 20.9 (*p*-C*C*H_3), 16.7 (*m*-C*C*H_3). Spectroscopic data for **2b** in $CDCl_3$ has been reported in literature.[11]

3.1.3 $[Au(IMes)_2]BPh_4$ (2c)

HIMes·BPh_4 (159 mg, 0.25 mmol). Crude product was dissolved in tetrahydrofuran (5 mL) and filtered through a glass microfibre filter in a Pasteur pipette to remove remaining copper compounds. Diethyl ether (30 mL) was added to the filtrated. The mixture was kept at 4 °C overnight. A white semi-crystalline solid was precipitated and solution decanted. Yield 90 %. **mp** 158 °C (dec.). **FT-IR** υ_{max} 3132 (w), 3053 (w), 2986 (w), 1732 (w), 1607 (w), 1581 (w), 1493 (m), 1424 (w), 1235 (m), 1033 (w), 854 (m), 727 (m), 706 (s), 606 (m) cm^{-1}. **MS**- ESI-TOF-MS(+) (m/z): found 805.3544 $C_{42}H_{48}AuN_4^+$ requires 805.3539. **^{1}H NMR** (600 MHz, DMSO-d_6) δ ppm 7.67 (s, 4H, NC*H*C*H*N), 7.15 - 7.20 (m, 8H, Ar*H*), 6.98 (s, 8H, BC_6H_5), 6.92 (t, 8H, BC_6H_5), 6.76 - 6.81 (m, 4H, BC_6H_5), 2.42 (s, 12H, *p*-CH_3), 1.65 ppm (s, 24H, *o*-CH_3).**^{13}C NMR** (151 MHz, DMSO-d_6) δ ppm 184.1 (N*C*N) 163.4 (q, $^1J_{BC}$ = 49.1 Hz, B*C*), 138.9 (Ar*C*), 135.6 (*o*-BPh_4), 134.1 (two overlapped Ar*C*), 128.7 (Ar*C*), 125.3 (q, *m*-

BPh_4), 123.5 (NCHCHN), 121.5 (*p*-BPh_4), 20.8 (*p*-CCH_3), 16.6 (*m*-CCH_3). Suitable crystals for X-ray diffraction were grown by slow evaporation from acetonitrile.

3.1.4 $[Au(ICy)_2]PF_6$ (2d)

$HICy{\cdot}PF_6$ (96 mg, 0.25 mmol). Crude product was dissolved in tetrahydrofuran (4 mL) and diethyl ether (15 mL) was added. The mixture was kept at 4 °C overnight and then decanted. A white precipitated was obtained and dried *in vacuum* to afford the desired product. Yield 87 %. **^{1}H NMR** (600 MHz, DMSO-d_6) δ ppm: 7.68 (s, 4H, NCHCHN), 4.46 (tt, 4H, NCHCH$_2$), 1.97-2.08 (m, 8H, CH$_2$), 1.79 - 1.92 (m, 16H, CH$_2$), 1.69 (d, 4H, CH$_2$), 1.30 - 1.43 (m, 8H, CH$_2$), 1.15 - 1.29 (m, 4H, CH$_2$). **^{13}C NMR** (151 MHz, DMSO-d_6) δ ppm 180.3 (NCN), 119.2 (NCHCHN), 60.6 (NCHCH$_2$), 33.4 (CH$_2$), 25.1 (CH$_2$), 24.5 (CH$_2$).

3.1.5 $[Au(ICy)_2]BF_4$ (2e)

$HICy{\cdot}BF_4$ (81 mg, 0.25 mmol). Crude product was purified by preparative thin layer chromatography (10:1 dichlormethane:acetonitrile as eluent) to obtain a white slightly yellow solid. R_f (10:1 dichlormethane:acetonitrile) 0.8. Yield 43 %. **mp** 180 °C (dec.). **FT-IR** υ_{max} 3131 (w), 3093 (w), 2929 (m), 2857 (m), 2144 (w), 1736 (m), 1562 (w), 1440 (m), 1247 (m), 1033 (s), 754 (m) cm^{-1}. **MS**- ESI-TOF-MS(+) (m/z): found 661.3549 $C_{30}H_{48}AuN_4^+$ requires 661.3539. **^{1}H NMR** (600 MHz, DMSO-d_6) δ ppm: 7.68 (s, 4H, NCHCHN), 4.45 (t, 4H, NCHCH$_2$), 1.96-2.09 (m, 8H, CH$_2$), 1.79 - 1.91 (m, 16H, CH$_2$), 1.69 (d, 4H, CH$_2$), 1.30 - 1.44 (m, 8H, CH$_2$), 1.21 (m, 4H, CH$_2$). **^{13}C NMR** (151 MHz, DMSO-d_6) δ ppm 180.4 (NCN), 119.3 (NCHCHN), 60.7 (NCHCH$_2$), 33.5 (CH$_2$), 25.2 (CH$_2$), 24.6 (CH$_2$). Suitable crystals for X-ray diffraction were grown by slow evaporation from dichloromethane.

3.1.6 $[Au(ICy)_2]BPh_4$ (2f)

$HICy{\cdot}BPh_4$ (140 mg, 0.25 mmol). Crude product was dissolved in tetrahydrofuran (5 mL) and filtered through a glass microfibre filter in a Pasteur pipette to remove remaining copper compounds. Diethyl ether (30 mL) was added to the filtrated. The mixture was kept at 4 °C overnight and then decanted. A white solid was obtained. Yield 60 %. **FT-IR** υ_{max} 3141 (w), 3055 (w), 2931 (m), 2855 (m), 1739 (w), 1579 (w), 1543 (w), 1479 (m), 1428 (m), 1269 (w), 1202 (w), 1033 (w), 889 (w), 730 (m), 696 (s), 606 (m) cm^{-1}. **MS**- ESI-TOF-MS(+) (m/z): found 661.3541 $C_{30}H_{48}AuN_4^+$ requires 661.3539. **^{1}H NMR** (600 MHz, DMSO-d_6) δ ppm 7.67 (s, 4H, NCHCHN), 7.15 - 7.21 (m, 8H, BC_6H_5), 6.90-6.93 (m, 8H, BC_6H_5), 6.75 - 6.81 (m, 4H, BC_6H_5), 4.39 - 4.51 (m, 4H, NCHCH$_2$), 1.98 - 2.08 (m, 8H, CH$_2$), 1.79 - 1.91 (m, 16H, CH$_2$), 1.69 (d, 4H, CH$_2$), 1.29 - 1.42 (m, 8H, CH$_2$), 1.17 - 1.27 (m, 4H, CH$_2$). **^{13}C NMR**

(151 MHz, DMSO-d_6) δ ppm 180.3 (N*C*N) 163.3 (q, $^1J_{BC}$ = 49.2 Hz, B*C*), 135.4 (*o*-BPh_4), 125.2 (t, *m*-BPh_4), 121.4 (*p*-BPh_4), 119.2 (N*C*H*C*HN), 60.6 (N*C*HCH$_2$), 33.4 (*C*H$_2$), 25.1 (*C*H$_2$), 24.4 (*C*H$_2$). Suitable crystals for X-ray diffraction were grown by slow evaporation from acetonitrile.

3.1.7 [Au(IEtMe)$_2$]PF$_6$ (2g)

HIEtMe·PF_6 (65 mg, 0.25 mmol). Crude product was washed with tetrahydrofuran (3 mL), kept at 4 °C overnight and then decanted. A white solid was obtained. Yield 81 %. **^{1}H NMR** (600 MHz, DMSO-d_6) δ ppm 7.58 (d, $^3J_{HH}$=2.1 Hz, 2H, NC*H*CHN), 7.49 (d, $^3J_{HH}$=2.1 Hz, 2H, NCHC*H*N), 4.23 (q, $^3J_{HH}$=7.6 Hz, 4H, CH_2), 3.85 (s, 6H, NCH_3), 1.43 (t, 6H, $^3J_{HH}$=7.6 Hz, CH_2CH_3). **^{13}C NMR** (151 MHz, DMSO-d_6) δ ppm 182.4 (N*C*N), 123.2 (N*C*HCHN), 121.5 (NCH*C*HN), 45.3 (N*C*H$_2$), 37.4 (N*C*H$_3$), 16.8 (CH_2CH_3). These data agreed with reported literature.[12]

3.1.8 [Au(IEtMe)$_2$]BF$_4$ (2h)

HIEtMe·BF_4 (51 mg, 0.25 mmol). Crude product was partially dissolved in tetrahydrofuran (2 mL) and diethyl ether (10 mL) was added. The mixture was kept at 4 °C for two hours and then decanted. A white precipitated was obtained and dried *in vacuum* to afford the desired product. Yield 80 %. **FT-IR** υ_{max} 3344 (w), 3170 (w), 3141 (w), 2974 (w), 1739 (w), 1567 (w), 1474 (m), 1445 (m), 1407 (w), 1340 (w), 1269 (w), 1219 (m), 1047 (s), 1033 (s), 732 (s), 694 (s) cm^{-1}. **MS**- ESI-TOF-MS(+) (m/z): found 417.1349 $C_{12}H_{20}AuN_4^+$ requires 417.1348. **^{1}H NMR** (600 MHz, DMSO-d_6) δ ppm 7.58 (d, $^3J_{HH}$=1.4 Hz, 2H, NC*H*CHN), 7.49 (d, $^3J_{HH}$=1.4 Hz, 2H, NCHC*H*N), 4.23 (q, $^3J_{HH}$=7.6 Hz, 4H, CH_2), 3.86 (s, 6H, NCH_3), 1.44 (t, $^3J_{HH}$=7.6 Hz, 6H, CH_2CH_3). **^{13}C NMR** (151 MHz, DMSO-d_6) δ ppm 182.4 (N*C*N), 123.2 (N*C*HCHN), 121.6 (NCH*C*HN), 45.3 (N*C*H$_2$), 37.4 (N*C*H$_3$), 16.8 (CH_2CH_3). Suitable crystals for X-ray diffraction were grown by slow evaporation from dichloromethane.

3.1.9 [Au(IEtMe)$_2$]BPh$_4$ (2i)

HIEtMe·BPh_4 (108 mg, 0.25 mmol). Crude product was dissolved in tetrahydrofuran (5 mL) and filtered through a glass microfibre filter in a Pasteur pipette to remove green and brown impurities. To the yellow filtrated diethyl ether was added (30 mL). The mixture was kept at 4 °C for 2 h and decanted. A white precipitated was obtained. The solid was dissolved in hot ethyl acetate (8 mL) with gentle heating and then kept at 4 °C overnight. Colorless crystals were obtained. Yield 38 %. Light-sensitive. **mp** 138-140 °C. **FT-IR** υ_{max} 3165 (w), 3053 (w), 2981 (w), 1741 (w), 1581 (w), 1564 (w), 1471 (m), 1405 (w), 1216 (m),

1035 (w), 842 (w), 732 (s), 706 (s), 610 (s) cm^{-1}. **MS**- ESI-TOF-MS(+) (m/z): found 417.1348 $C_{12}H_{20}AuN_4^+$ requires 417.1348. **^{1}H NMR** (600 MHz, DMSO-d_6) δ ppm 7.56 - 7.58 (m, 2H, NC*H*CHN), 7.47 – 7.48 (m, 2H, NCHC*H*N), 7.12 - 7.20 (m, 8H, BC_6H_5), 6.90 – 6.94 (m, 8H, BC_6H_5), 6.77 – 6.80 (m, 4H, BC_6H_5), 4.22 (q, $^3J_{HH}$=7.2 Hz, 4H, CH_2), 3.84 (s, 6H, NCH_3), 1.42 (t, $^3J_{HH}$=7.2 Hz, 6H, CH_2CH_3). **^{13}C NMR** (151 MHz, DMSO-d_6) δ ppm 182.5 (N*C*N) 163.3 (q, $^1J_{BC}$ = 49.1 Hz, B*C*), 135.5 (*o*-BPh_4), 125.3 (q, *m*-BPh_4), 123.3 (NCHCHN), 121.6 (NCH*C*HN), 121.5 (*p*-BPh_4), 45.4 (NCH_2), 37.5 (NCH_3), 16.9 (CH_2CH_3). Suitable crystals for X-ray diffraction were grown by slow evaporation from acetonitrile.

4. $[Cu(NHC)_2]^+$ as a transmetalation agent for $[Au(NHC)_2]^+$

To evidence the presence of bis(NHC)-Cu(I) complexes and examine their role as transmetalation agents in the proposed reaction system, three experiments with ligand **1a** were carried out:

a) Powdered gold (12.5 mg, 0.06 mmol, purity ≥ 99.9 %, size < 10 μm), ligand **1a** (0.12 mmol), acetonitrile (7.5 mL), $CuSO_4$ (250 μL, 0.5 M, 0.12 mmol), and aqueous ammonia solution (5 mL, 28 %) were added to a pressure tube. The mixture was stirred in an oil bath at 80 °C for *30 min*.

b) Same procedure as **a**) but stirred for *60 min*.

c) Same procedure as **a**) but *without gold*.

After the stated time, the reaction mixture was allowed to cool to room temperature. One milliliter of each solution was taken directly and filtered through a nylon membrane (0.20 μm pore diameter). Then, the solutions were analyzed by mass spectrometry.

a)

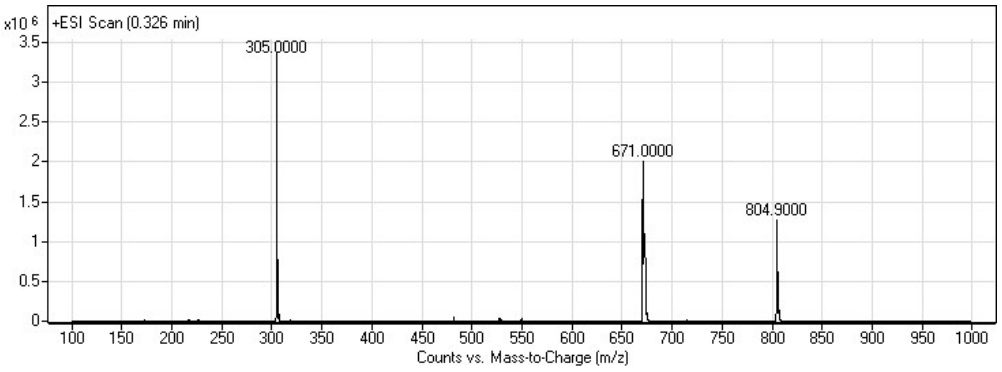

b)

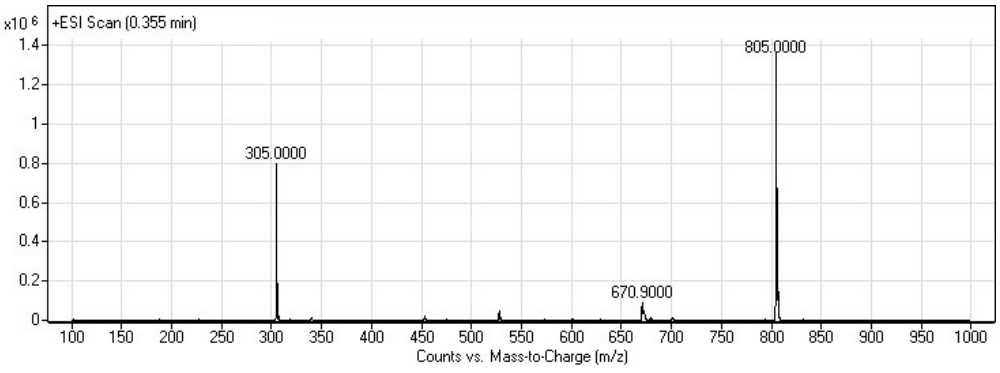

c)

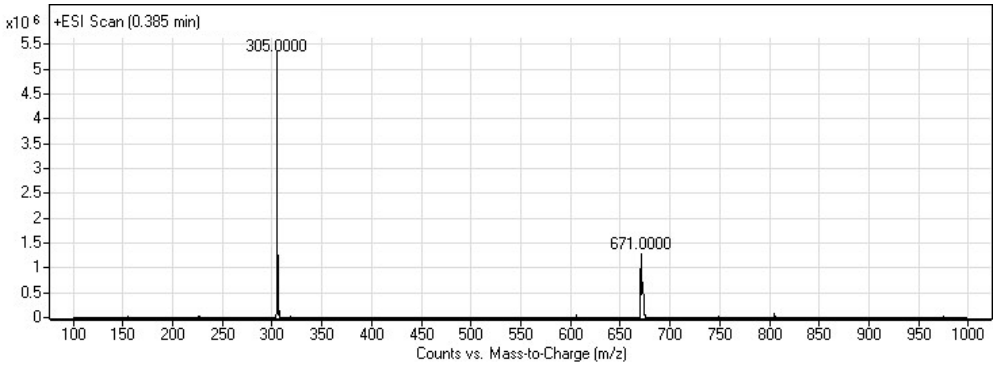

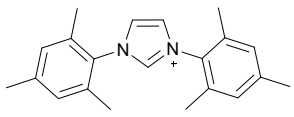

Exact Mass: 305.2012

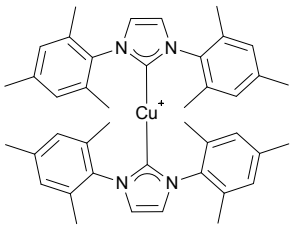

Exact Mass: 671.3170

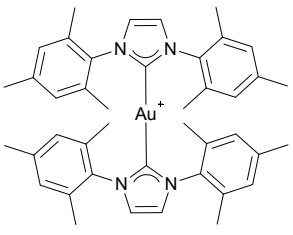

Exact Mass: 805.3539

Figure 1. Mass spectra for experiments **a**) With gold, 30 min of reaction. **b**) With gold, 60 min of reaction. **c**) Without gold, 30 min of reaction.

5. Halogens as counterions.

The preparation of the bis(NHC)-Au(I) complex with counterions such as Cl^- (HIMes·Cl and HICy·Cl) and Br^- (HIEtMe·Br) was examined with the methodology proposed. Nevertheless the molar ratio of gold to imidazolium salt used, mixtures of mono and bis(NHC)-Au(I) complexes were obtained. As an example, the ^{1}H-NMR spectrum of the crude mixture of the corresponding reaction with two equivalents of HIMes·Cl is shown in Figure 2. The data is in accordance to reported literature.[13]

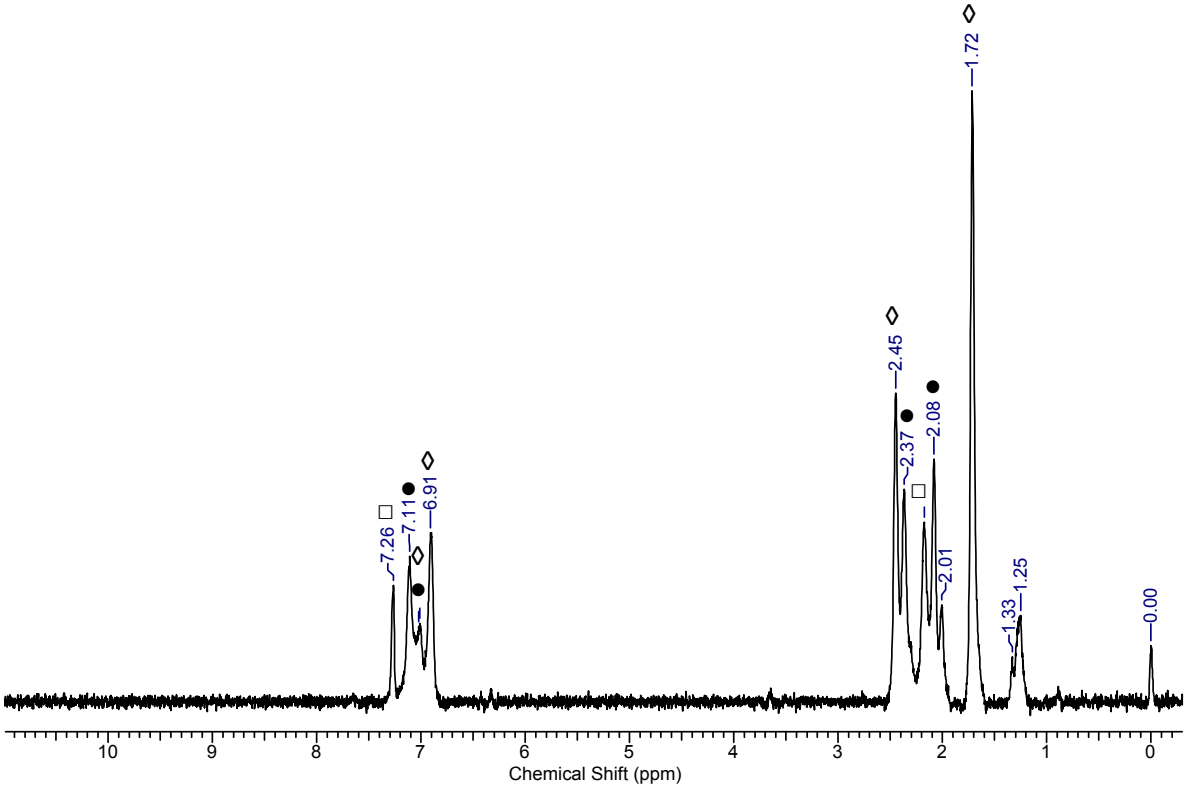

Figure 2. ^{1}H-NMR spectrum of the crude mixture of $[Au(IMes)_2]Cl$ (◊) and IMesAuCl (●) complexes, and HIMes·Cl ligand (□) in $CDCl_3$, 60 MHz.

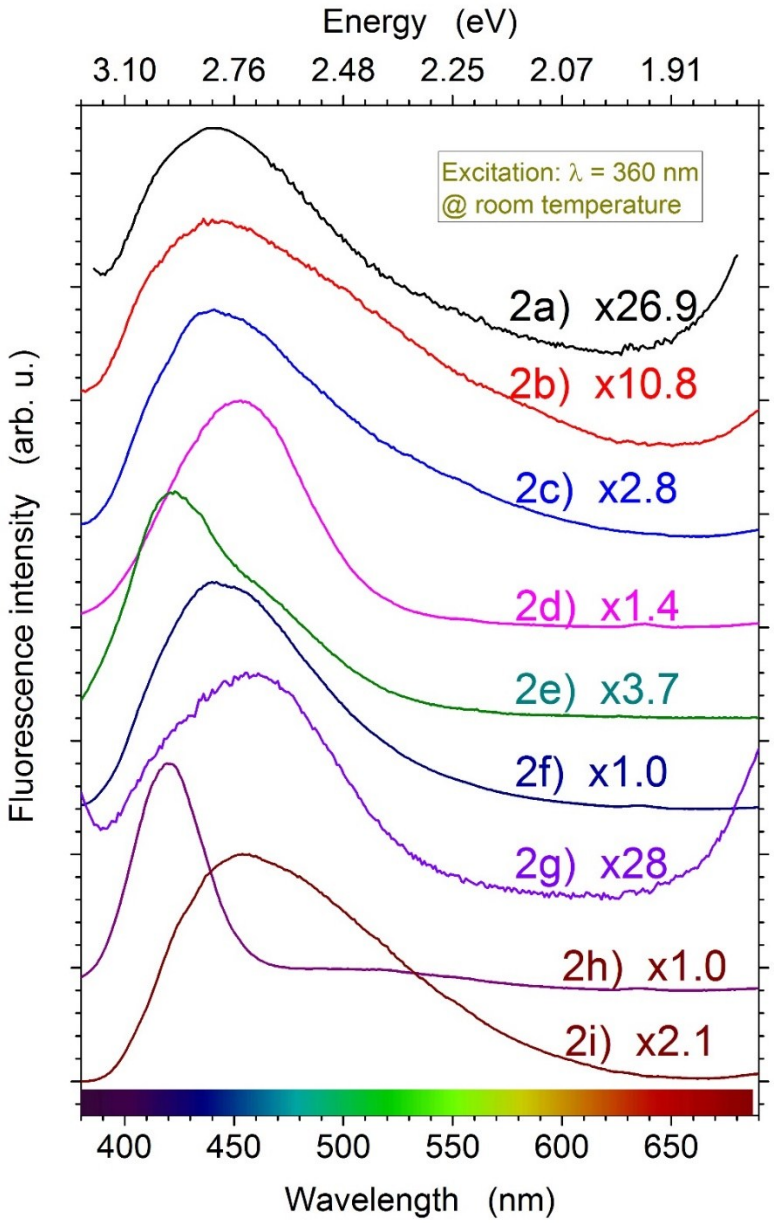

Figure 3. Emission spectra of compounds **2a-i** at λ_{ex}=360 nm.
The spectra were normalized, where "xN" represents the multiplier factor.
In this way the highest and lowest intensity were observed in the samples **2h** and **2g**, respectively.

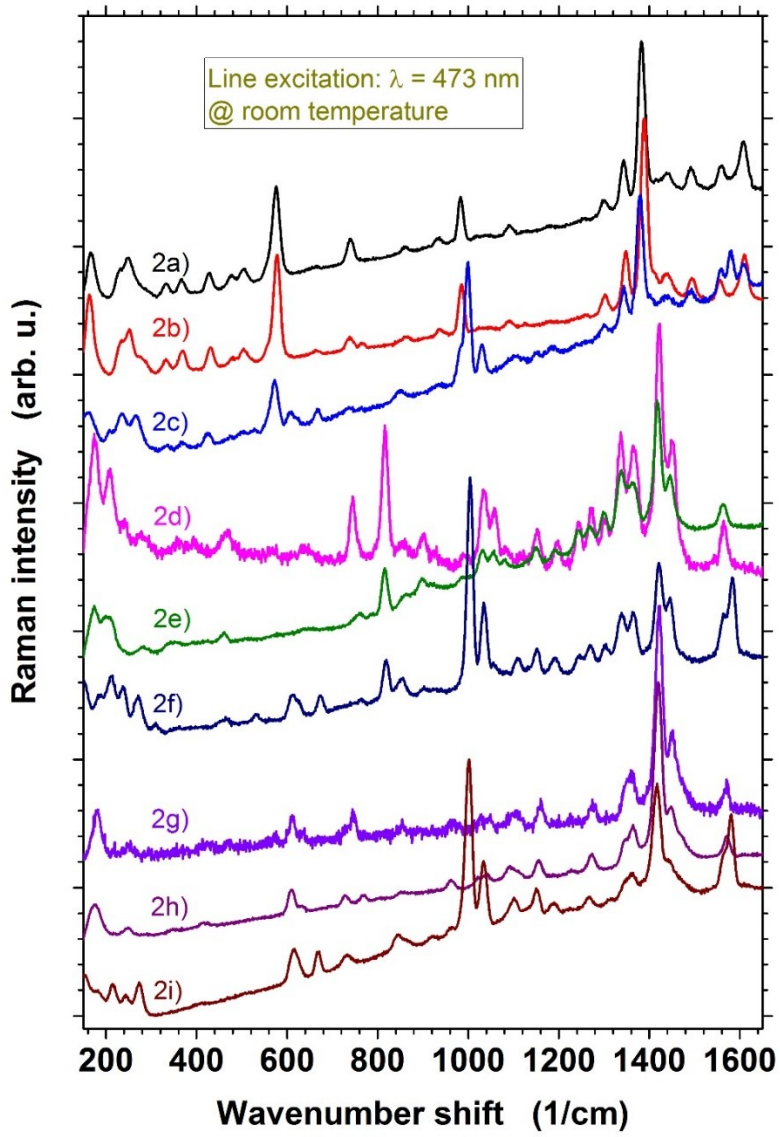

Figure 4. Raman spectra of compounds **2a**-**2i**.

The Raman spectra for complexes **2a**-**2i** are depicted in the Figure 4. It can be observed that some peaks are characteristic according to ligand and counterion present in the complex. A strong peak around 576 and 1610 cm^{-1} appear when $[Au(IMes)_2]^+$ is present, as can be observed for complexes **2a**, **2b** and **2c**; in the case of $[Au(ICy)_2]^+$, a characteristic peak appears around 816 cm^{-1}, as can be noticed for the samples **2d**, **2e** and **2f**; meanwhile, there is not a defined peak that could be clearly associated with $[Au(IEtMe)_2]^+$ at glance, as can be perceived for complexes **2g**, **2h** and **2i**. On the other hand, a peak around 744 cm^{-1} is observed when PF_6^- is present, as in compounds **2a**, **2d** and **2g**; a small peak around 768 cm^{-1} comes out only in the samples **2b**, **2e**, and **2h**, therefore it can be related to BF_4^-. Finally, an intensity double-peak at 1002 and 1034 cm^{-1} can be related to the BPh_4^-, because it is observed in complexes **2c**, **2f** and **2i**

5. NMR spectra

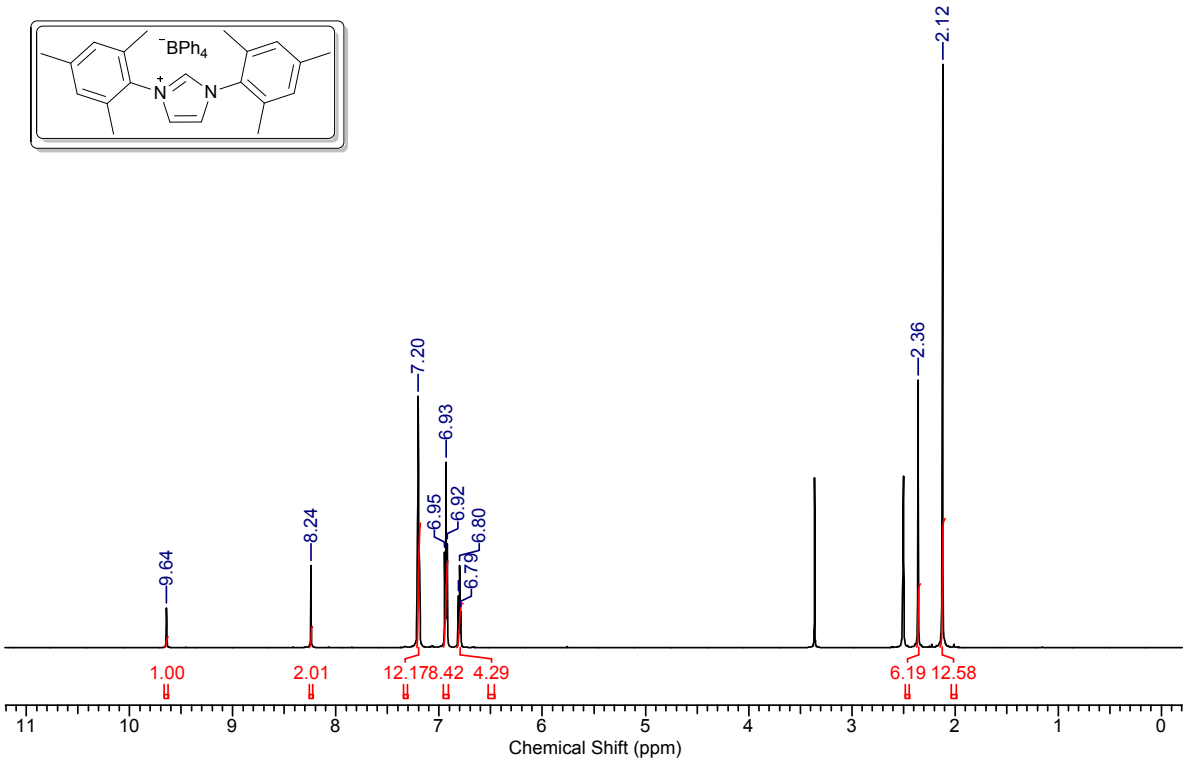

Figure 5. ^{1}H-NMR spectrum of HIMes·BPh_4 (**1c**) in DMSO-d6, 600 MHz.

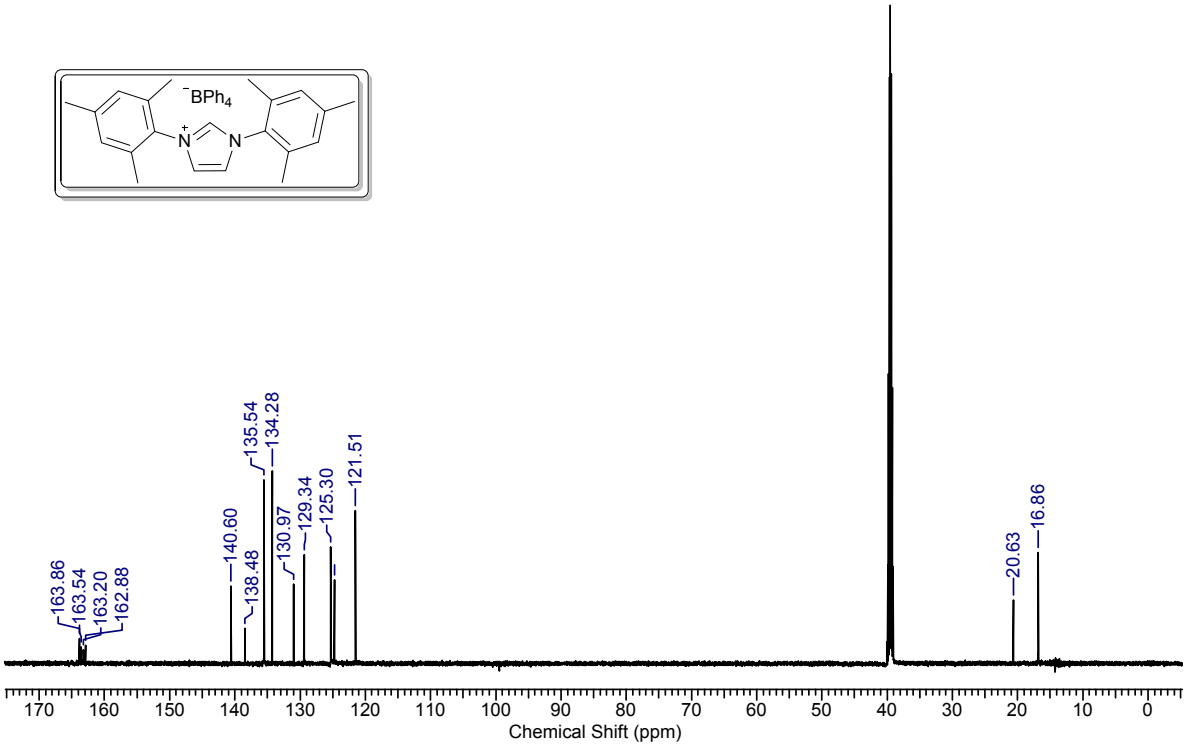

Figure 6. ^{13}C-NMR spectrum of HIMes·BPh_4 (**1c**) in DMSO-*d6*, 151 MHz.

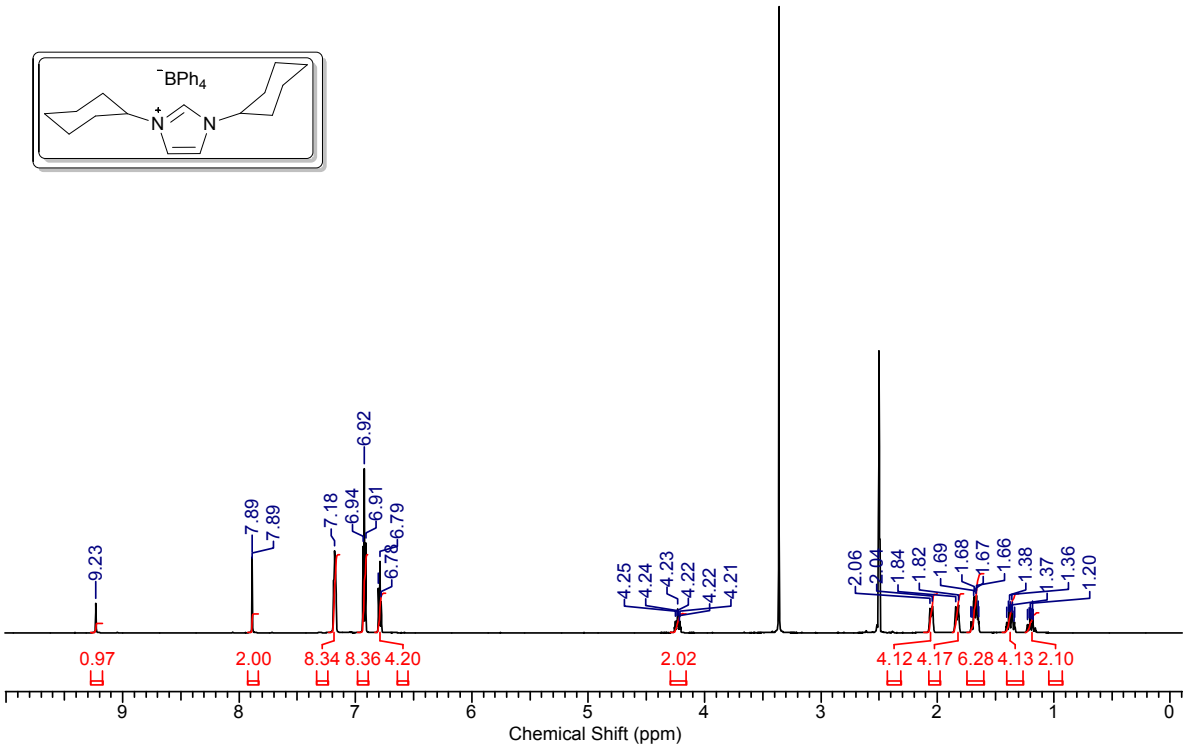

Figure 7. ^{1}H-NMR spectrum of HICy·BPh_4 (**1f**) in DMSO-*d6*, 600 MHz.

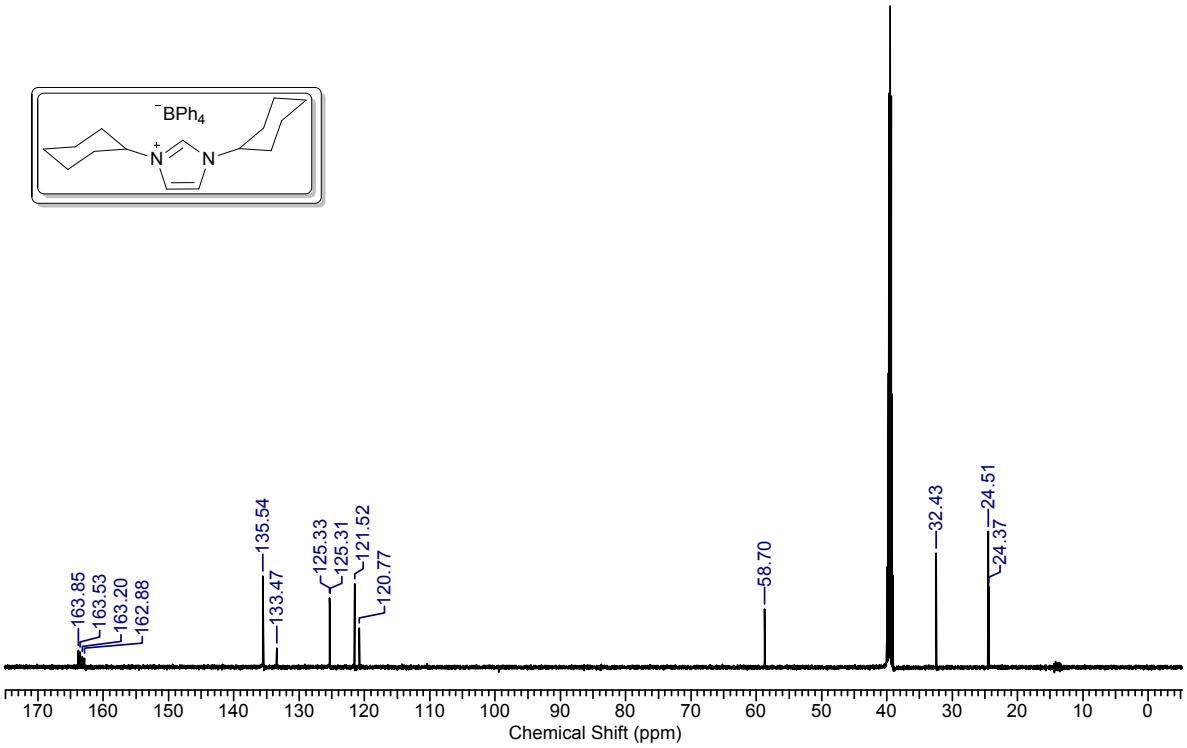

Figure 8. ^{13}C-NMR spectrum of HICy·BPh_4 (**1f**) in DMSO-*d6*, 151 MHz.

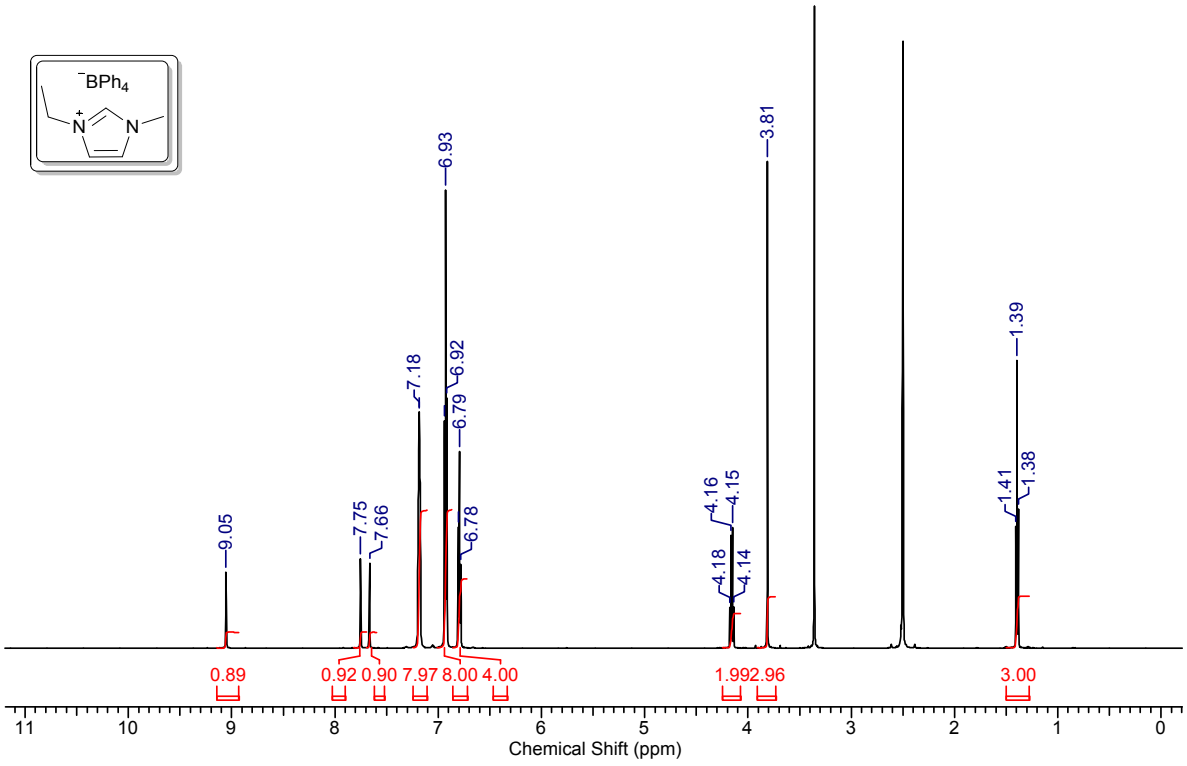

Figure 9. ^{1}H-NMR spectrum of HIEtMe·BPh_4 (**1i**) in DMSO-*d6*, 600 MHz.

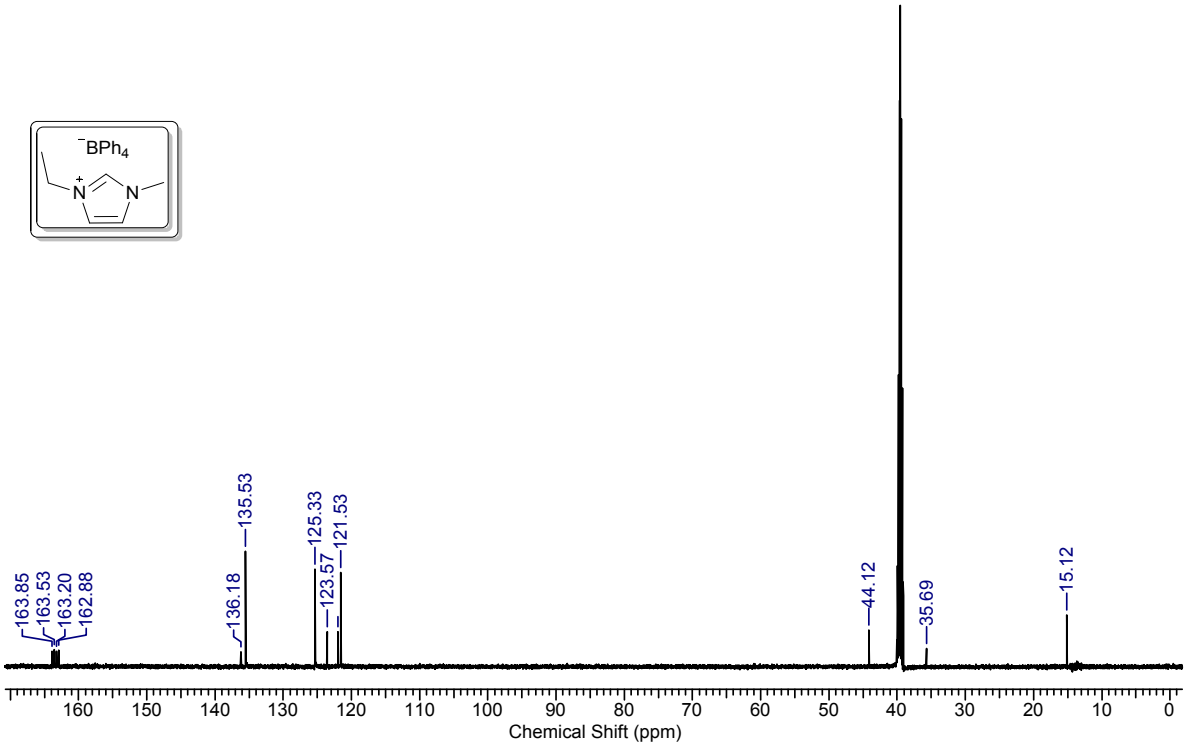

Figure 10. ^{13}C-NMR spectrum of HIEtMe·BPh_4 (**1i**) in DMSO-*d6*, 151 MHz.

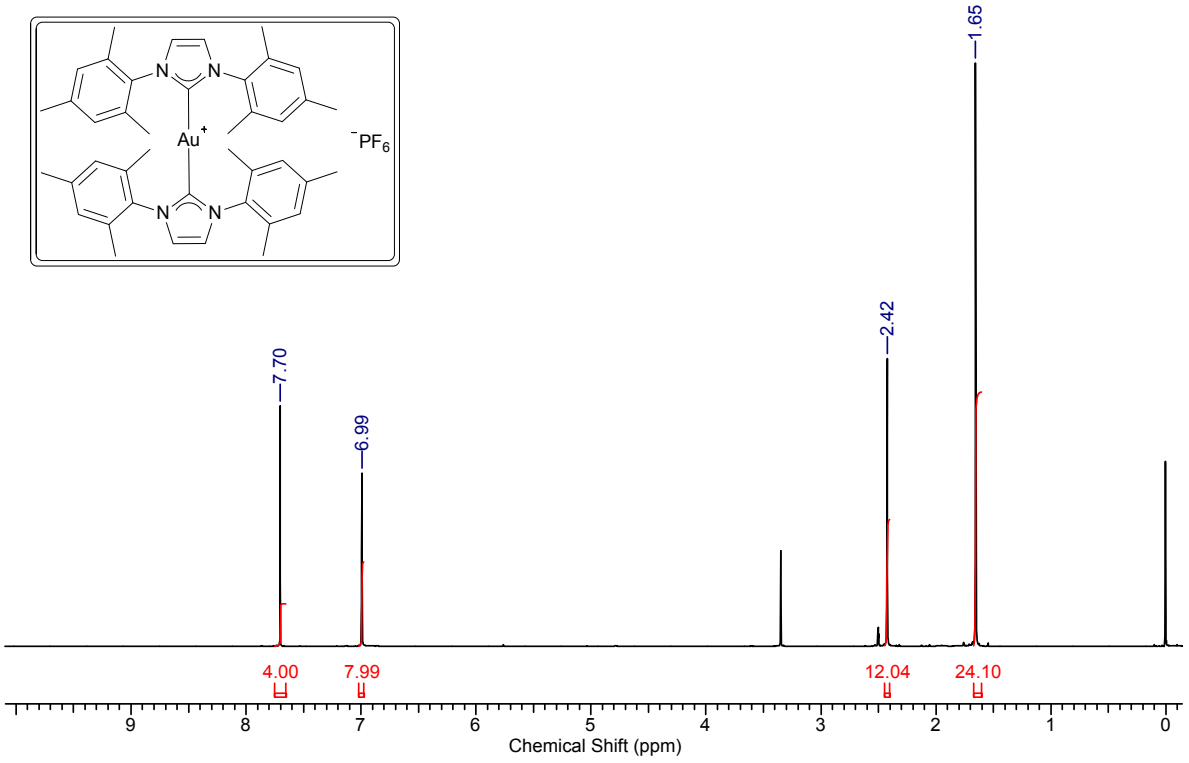

Figure 11. ^{1}H-NMR spectrum of [Au(IMes)$_2$]PF$_6$ (**2a**) in DMSO-*d6*, 600 MHz.

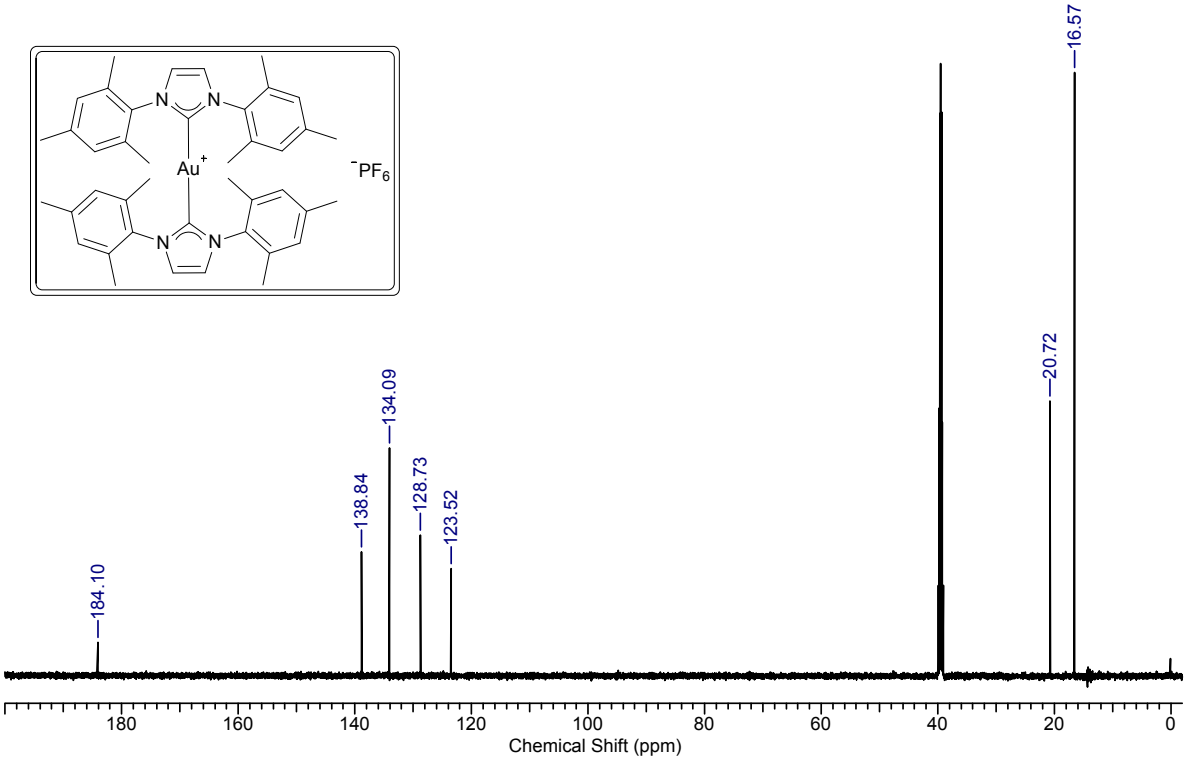

Figure 12. ^{13}C-NMR spectrum of [Au(IMes)$_2$]PF$_6$ (**2a**) in DMSO-*d6*, 151 MHz.

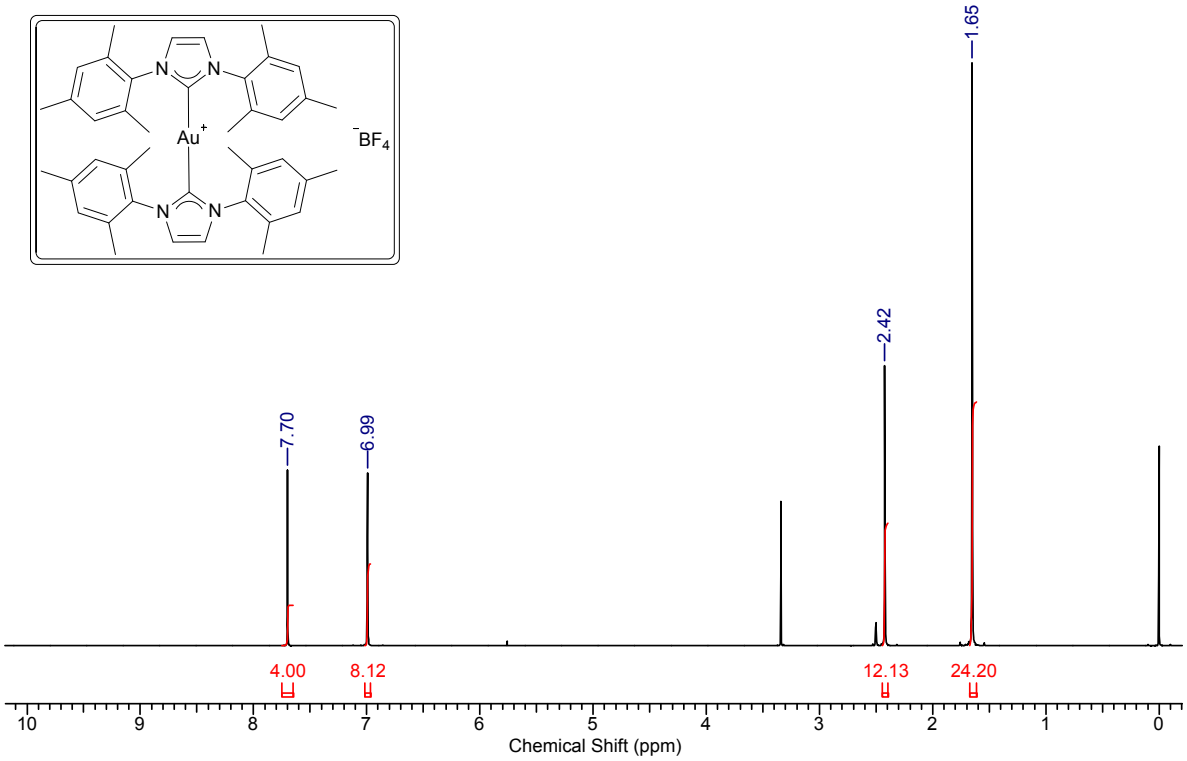

Figure 13. ^{1}H-NMR spectrum of [Au(IMes)$_2$]BF$_4$ (**2b**) in DMSO-*d6*, 600 MHz.

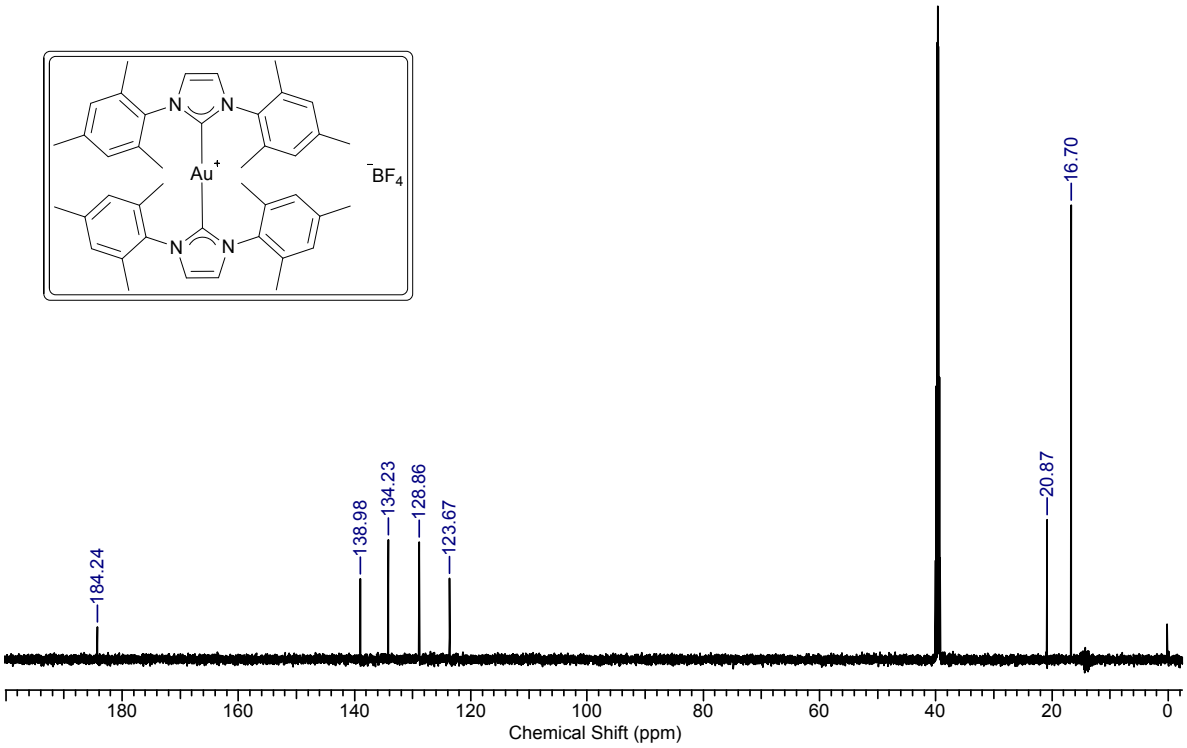

Figure 14. ^{13}C-NMR spectrum of [Au(IMes)$_2$]BF$_4$ (**2b**) in DMSO-*d6*, 151 MHz.

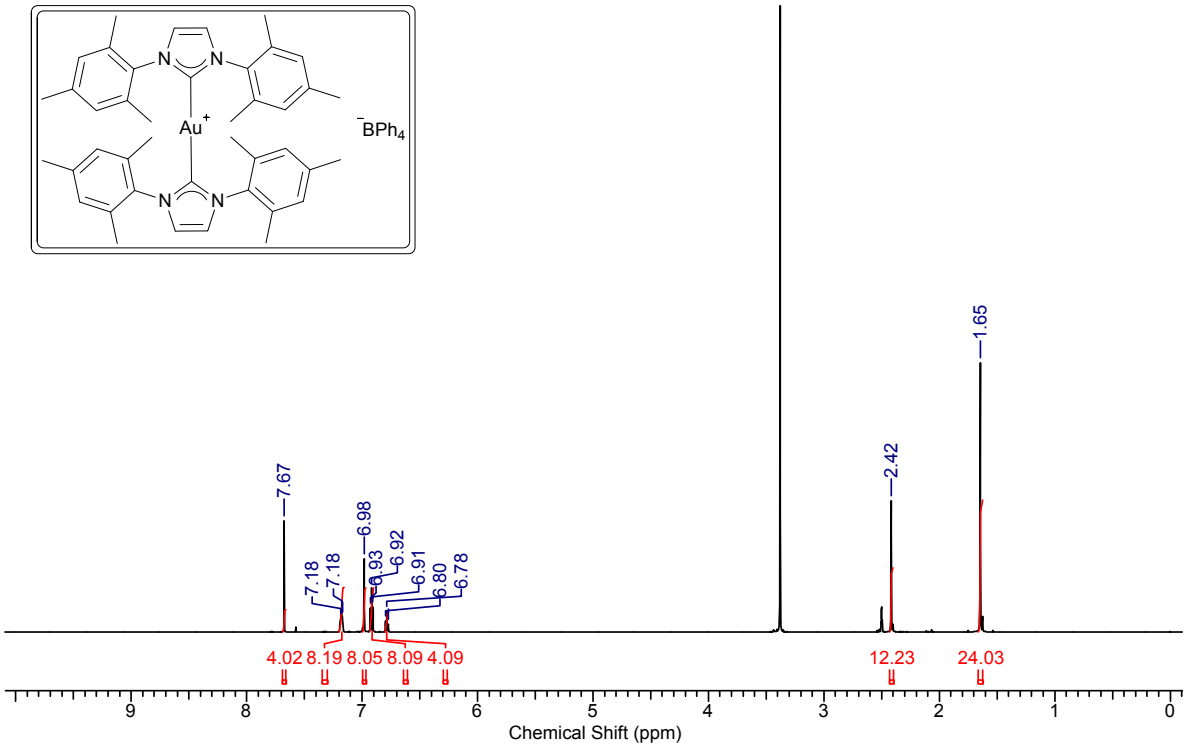

Figure 15. ^{1}H-NMR spectrum of [Au(IMes)$_2$]BPh$_4$ (**2c**) in DMSO-*d6*, 600 MHz.

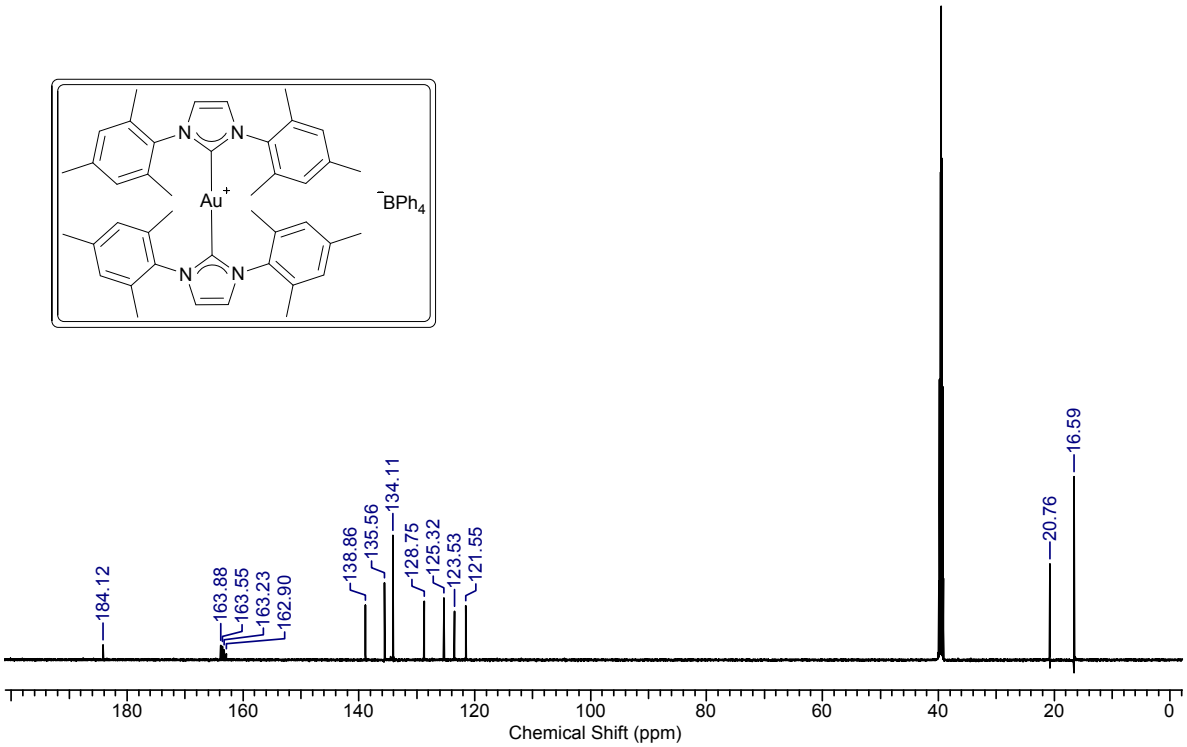

Figure 16. ^{13}C-NMR spectrum of [Au(IMes)$_2$]BPh$_4$ (**2c**) in DMSO-*d6*, 151 MHz.

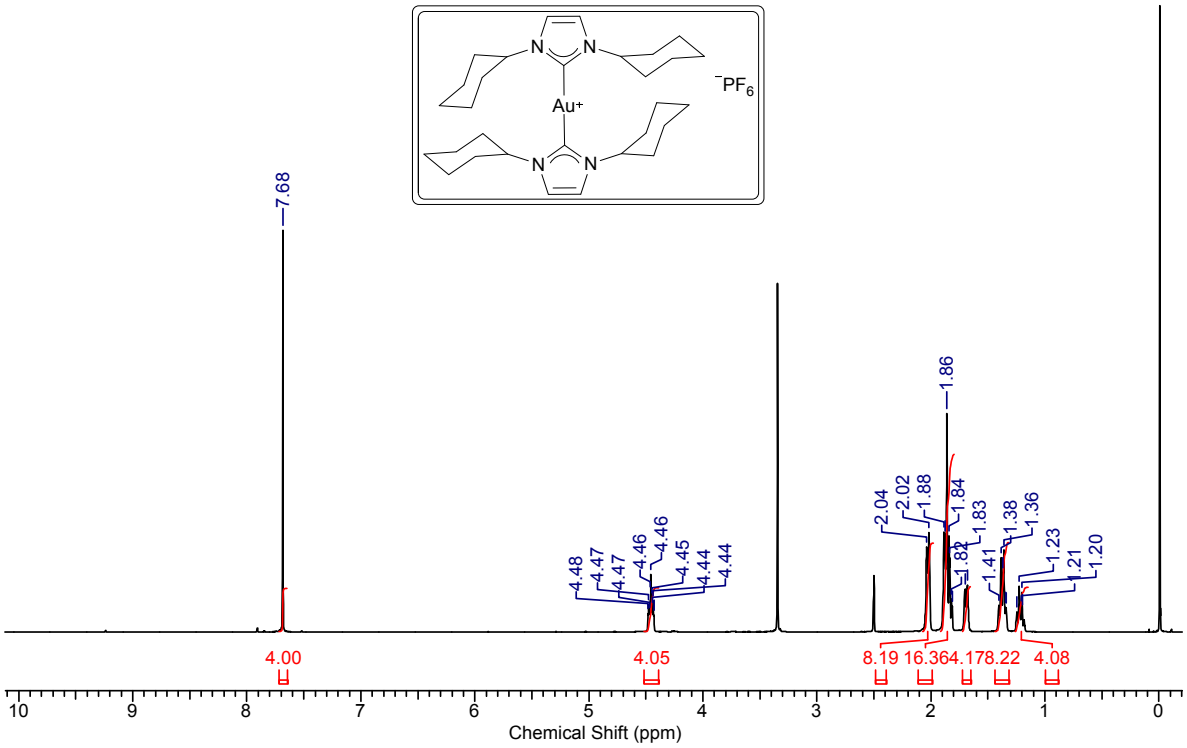

Figure 17. ^{1}H-NMR spectrum of $[Au(ICy)_2]PF_6$ (**2d**) in DMSO-*d6*, 600 MHz.

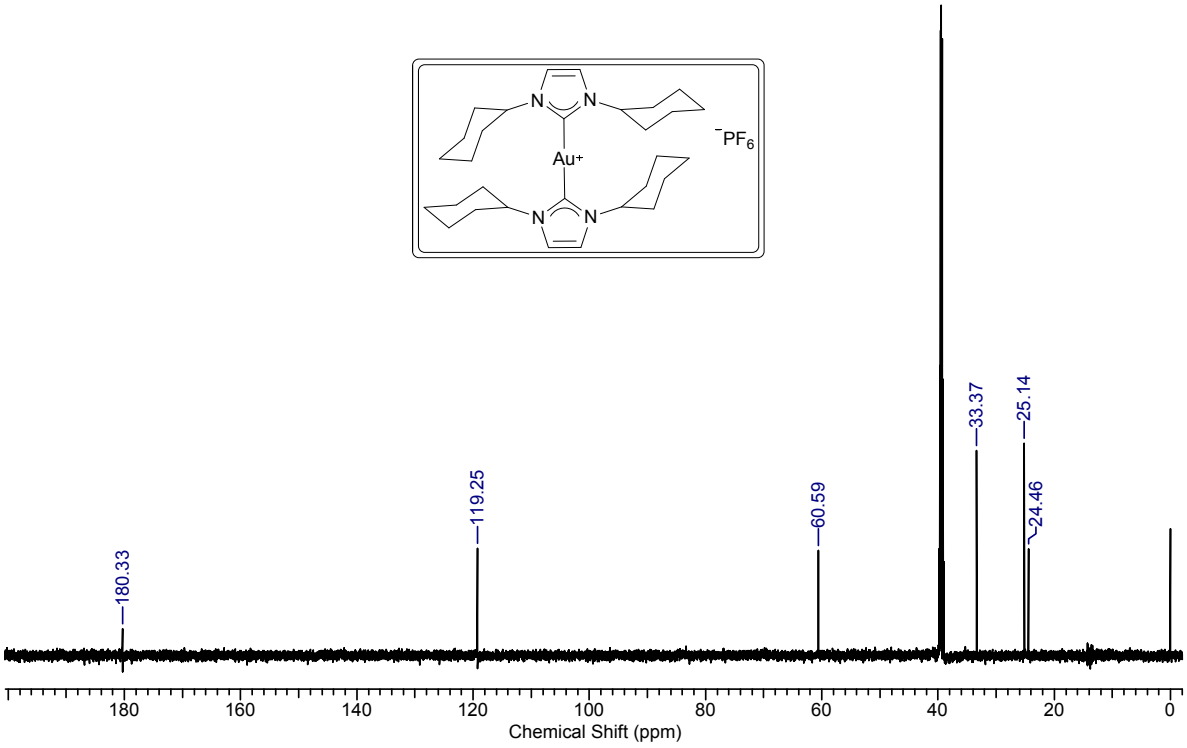

Figure 18. ^{13}C-NMR spectrum of $[Au(ICy)_2]PF_6$ (**2d**) in DMSO-*d6*, 151 MHz.

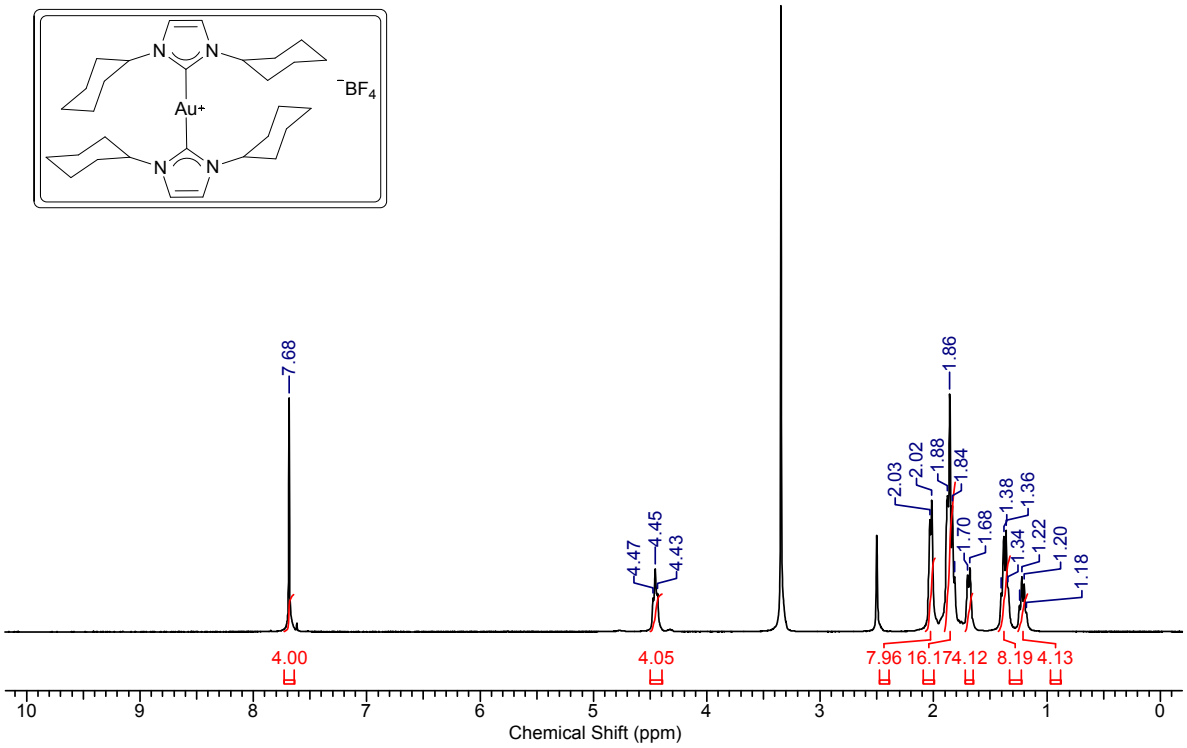

Figure 19. ^{1}H-NMR spectrum of [Au(ICy)$_2$]BF$_4$ (**2e**) in DMSO-*d6*, 600 MHz.

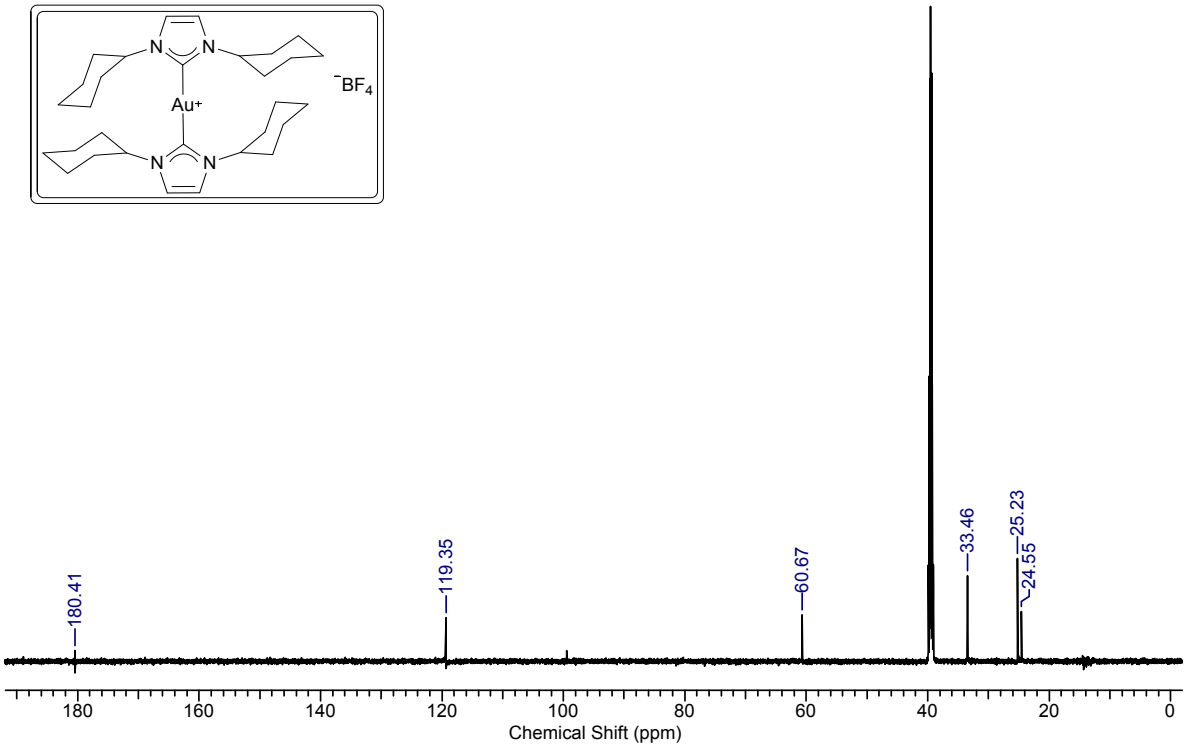

Figure 20. ^{13}C-NMR spectrum of [Au(ICy)$_2$]BF$_4$ (**2e**) in DMSO-*d6*, 151 MHz.

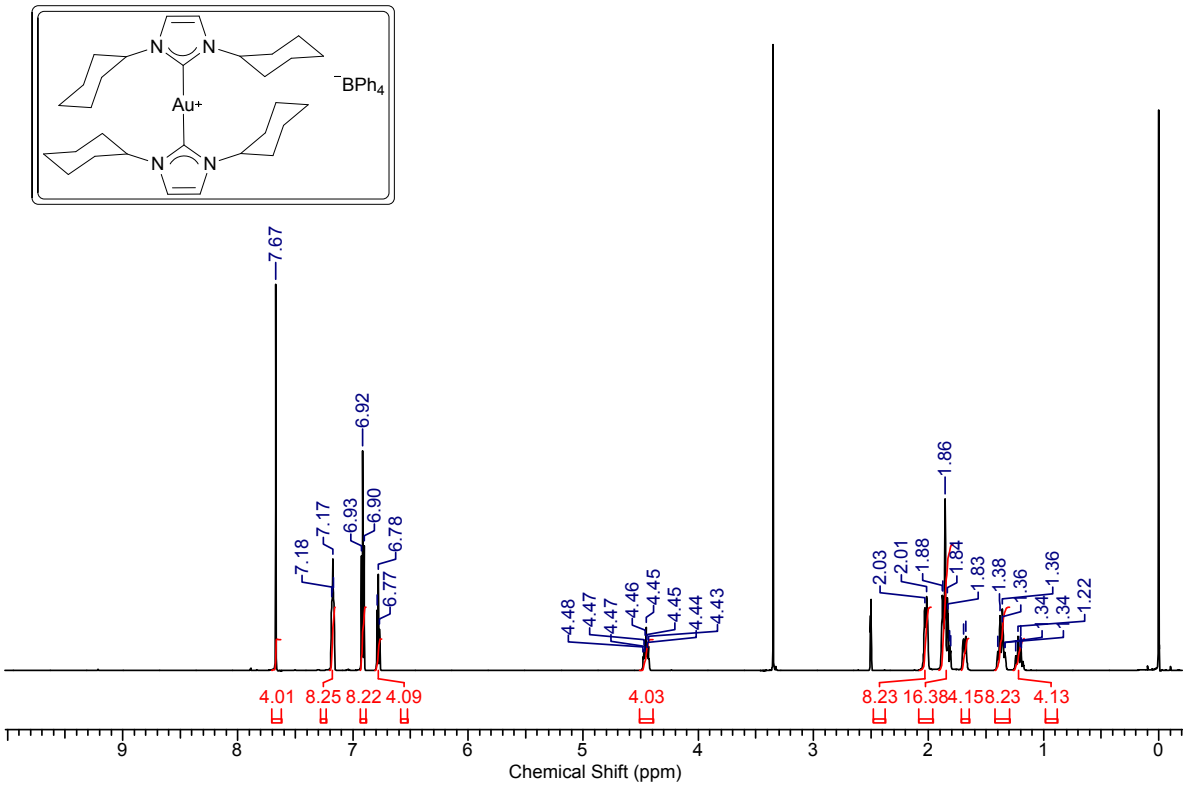

Figure 21. ^{1}H-NMR spectrum of $[Au(ICy)_2]BPh_4$ (**2f**) in DMSO-*d6*, 600 MHz.

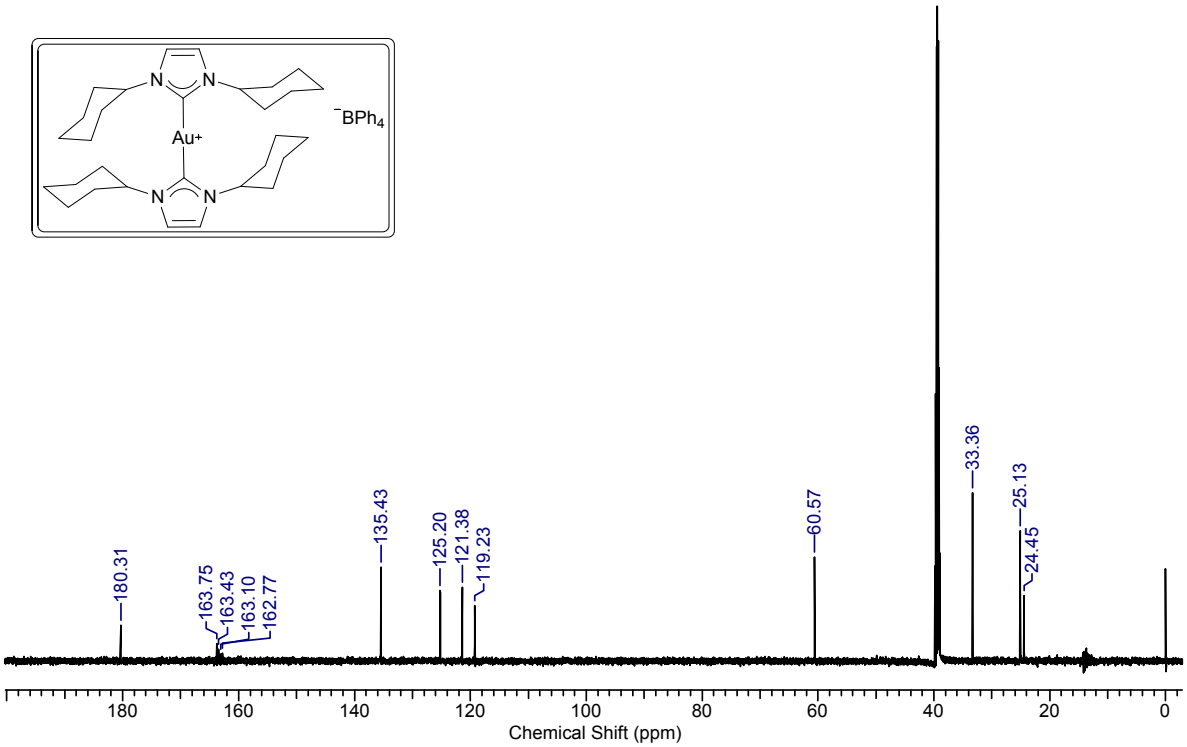

Figure 22. ^{13}C-NMR spectrum of $[Au(ICy)_2]BPh_4$ (**2f**) in DMSO-*d6*, 151 MHz.

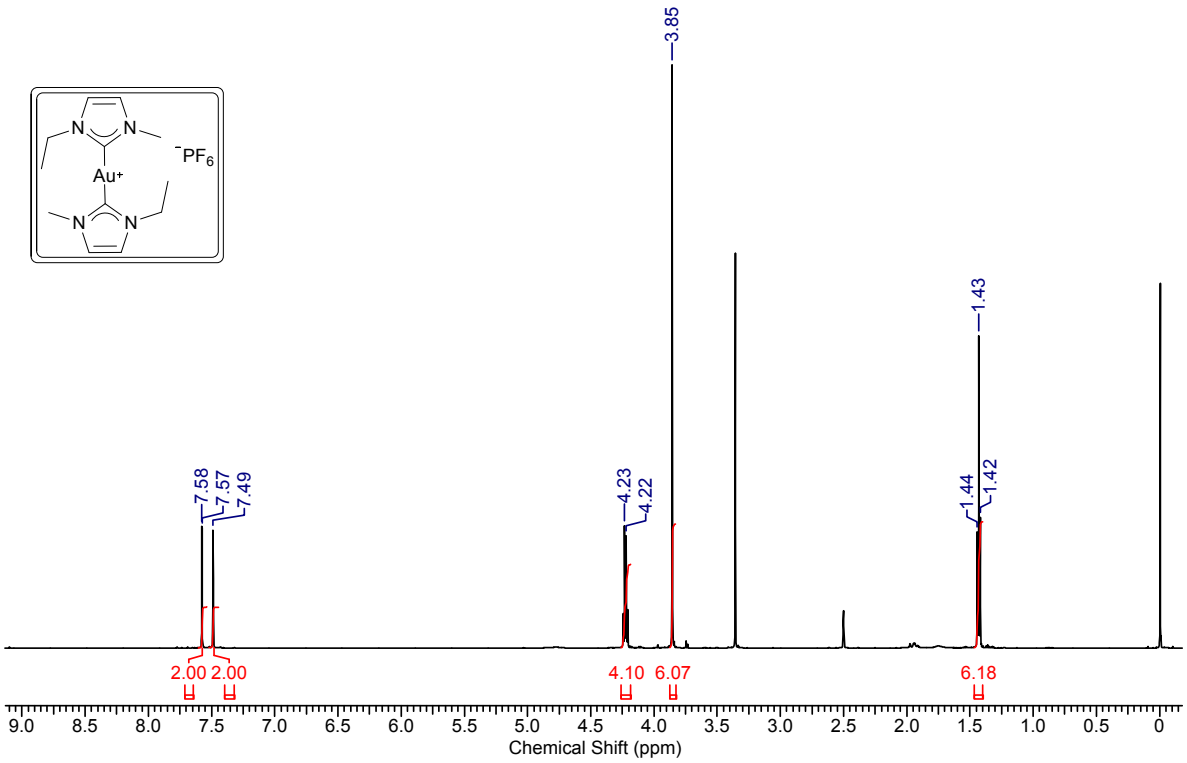

Figure 23. ^{1}H-NMR spectrum of [Au(IEtMe)$_2$]PF$_6$ (**2g**) in DMSO-*d6*, 600 MHz.

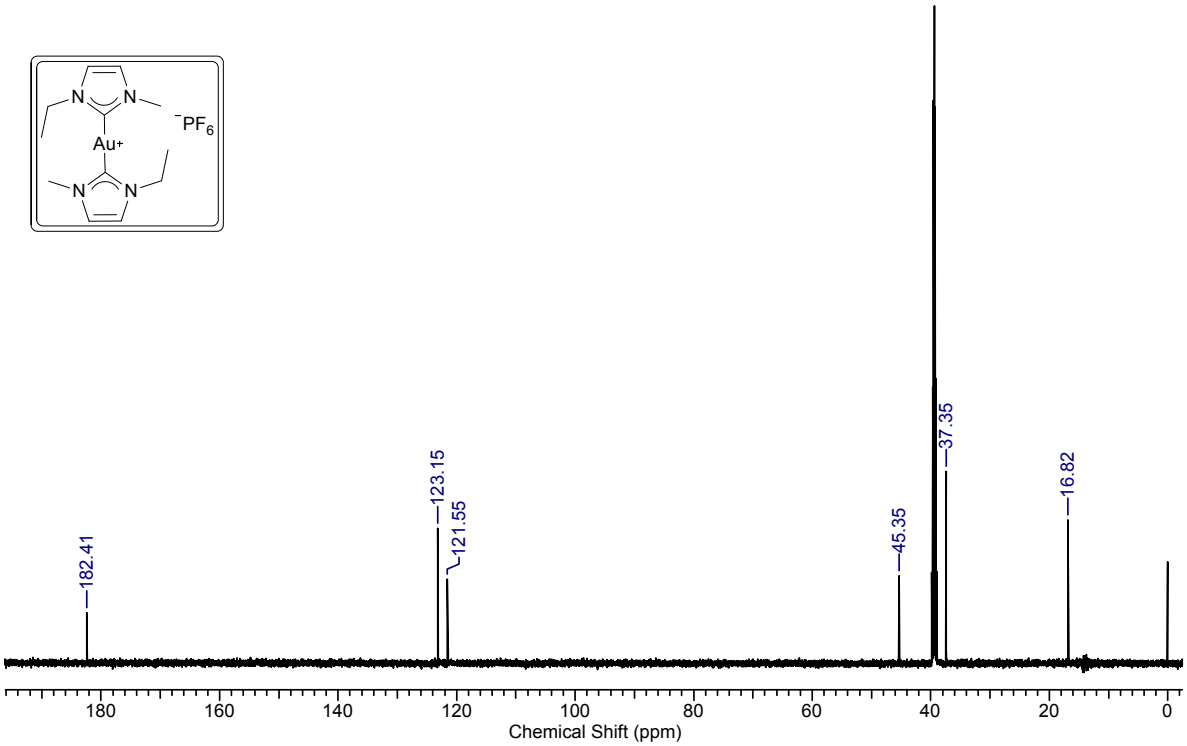

Figure 24. ^{13}C-NMR spectrum of [Au(IEtMe)$_2$]PF$_6$ (**2g**) in DMSO-*d6*, 151 MHz.

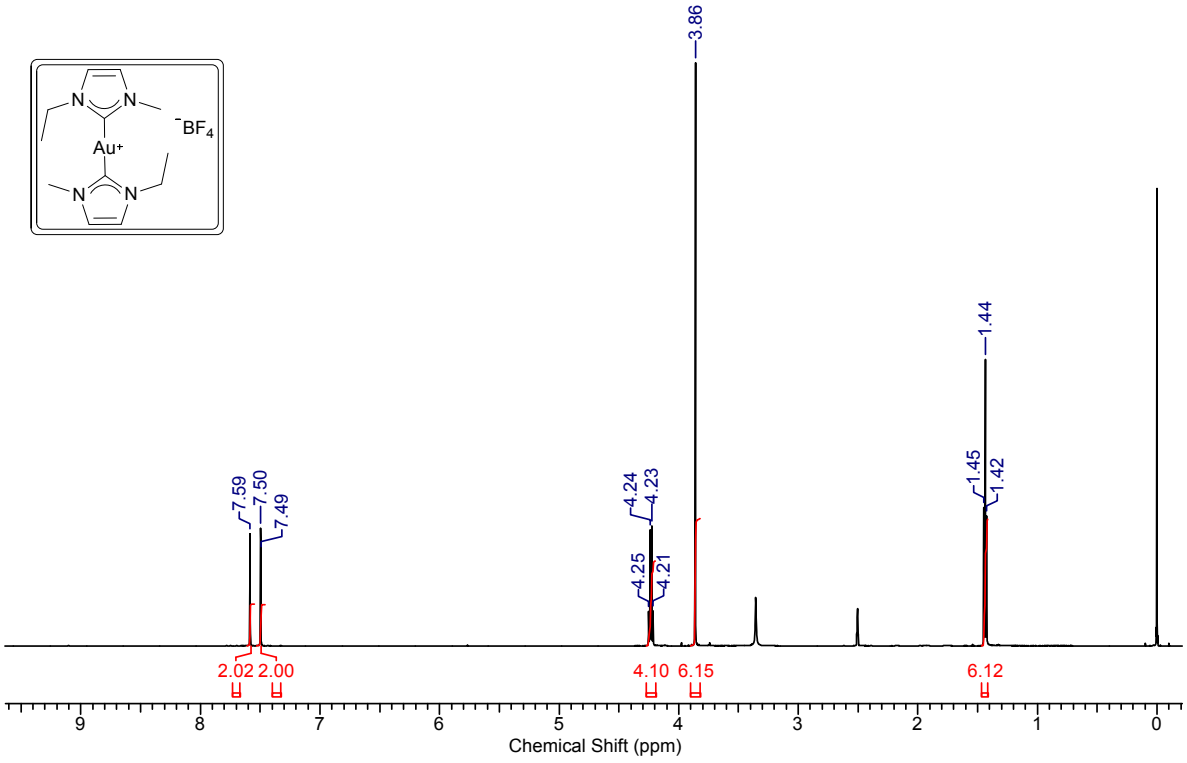

Figure 25. ^{1}H-NMR spectrum of [Au(IEtMe)$_2$]BF$_4$ (**2h**) in DMSO-*d6*, 600 MHz.

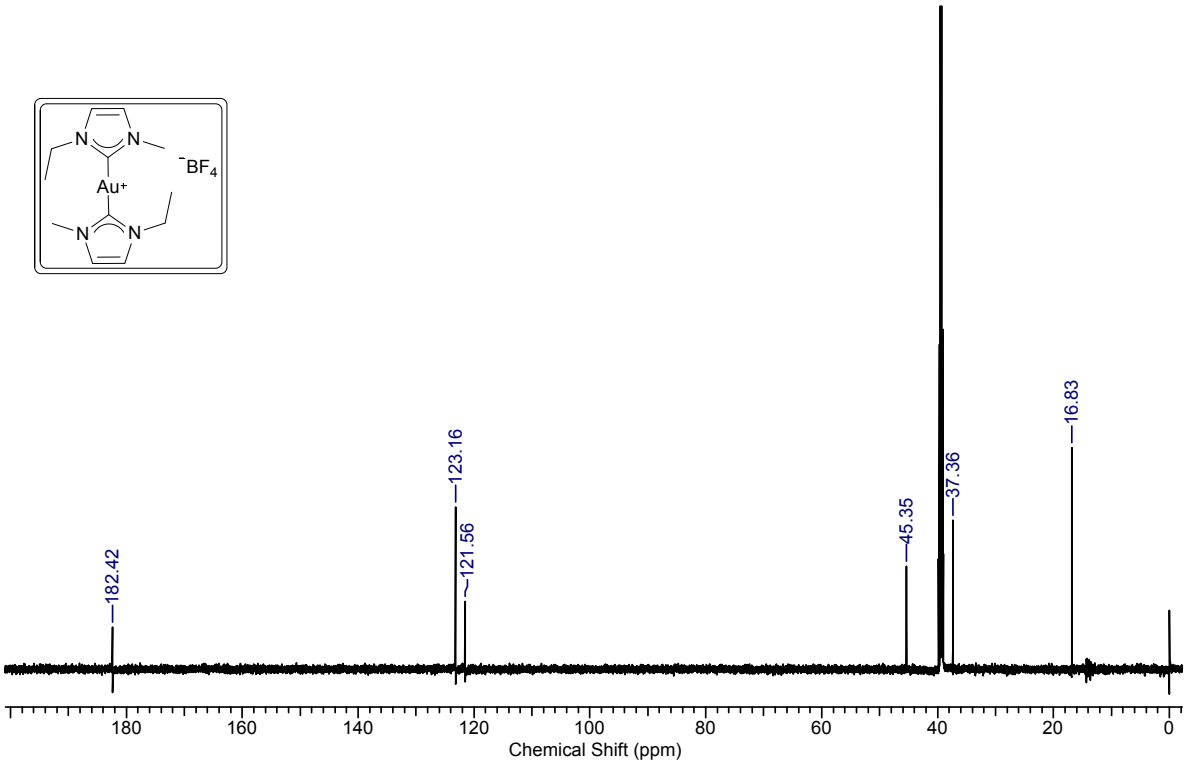

Figure 26. ^{13}C-NMR spectrum of [Au(IEtMe)$_2$]BF$_4$ (**2h**) in DMSO-*d6*, 151 MHz.

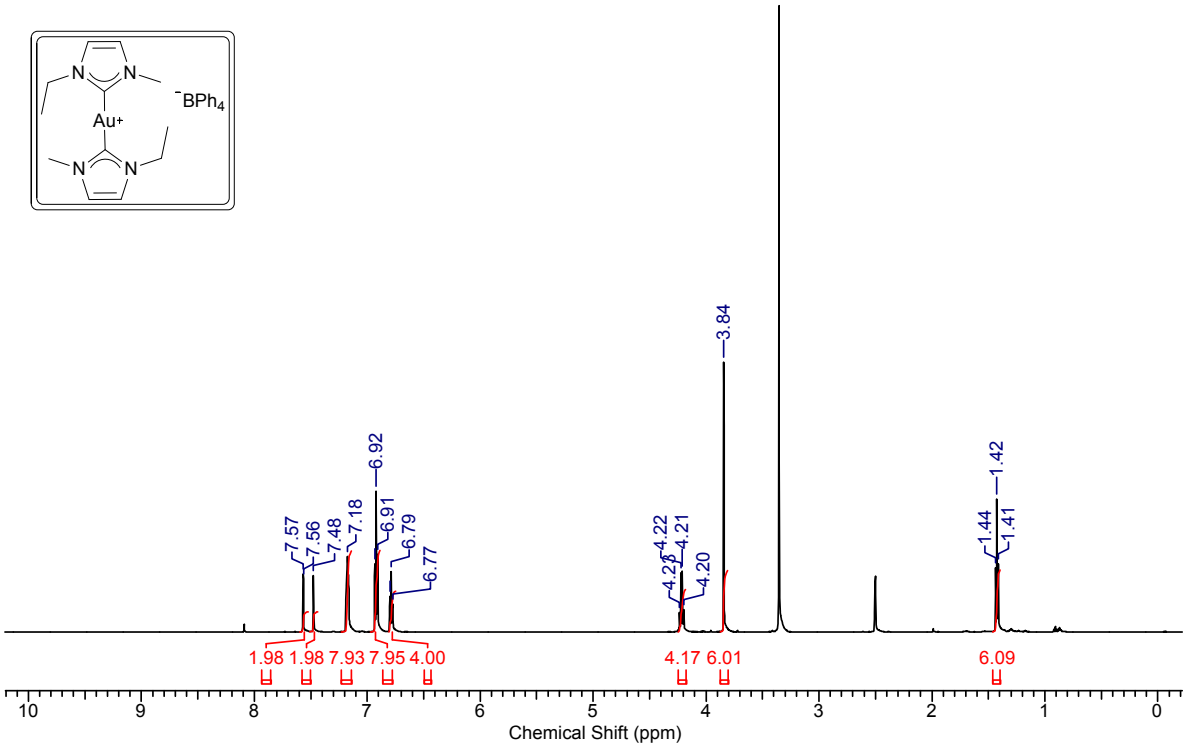

Figure 27. ^{1}H-NMR spectrum of [Au(IEtMe)$_2$]BPh$_4$ (**2i**) in DMSO-*d6*, 600 MHz.

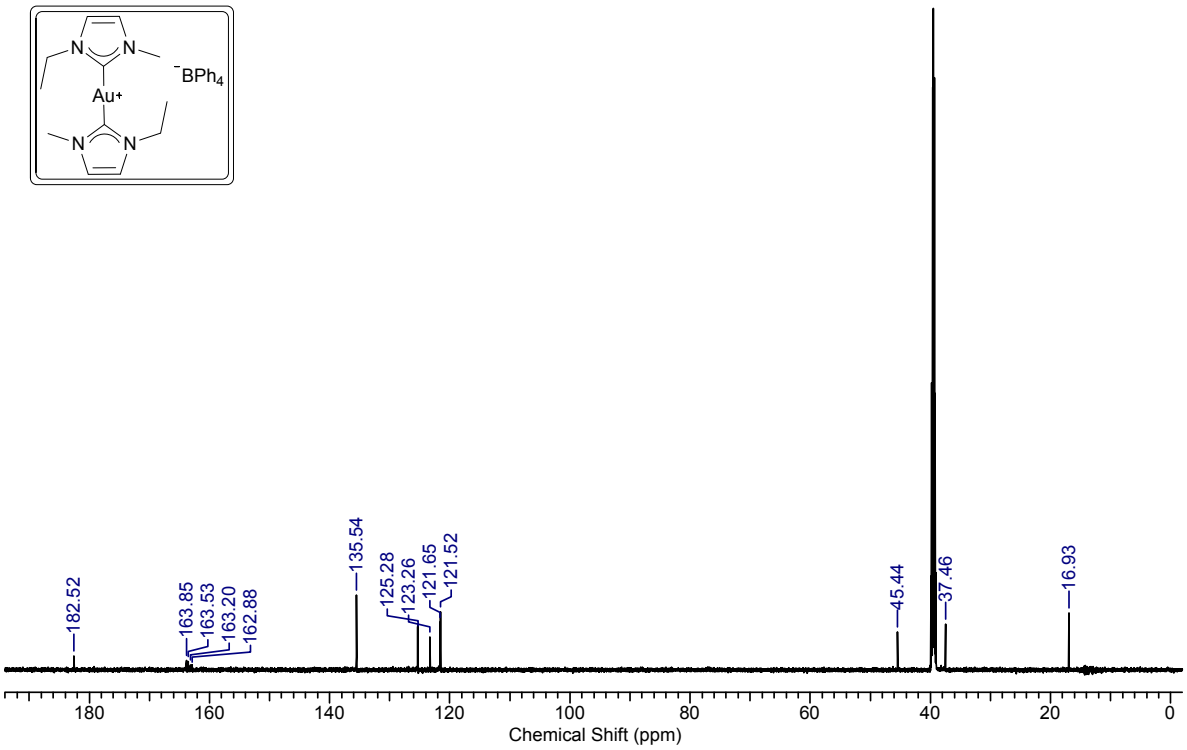

Figure 28. ^{13}C-NMR spectrum of [Au(IEtMe)$_2$]BPh$_4$ (**2i**) in DMSO-*d6*, 151 MHz.

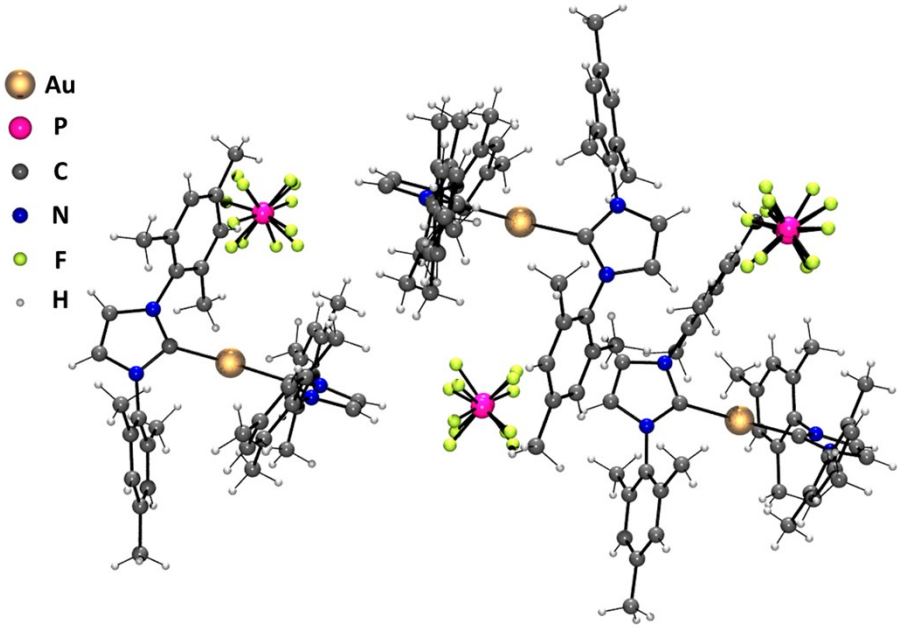

Figure 29. Crystal structure of $[Au(IMes)_2]PF_6$ (**2a**).

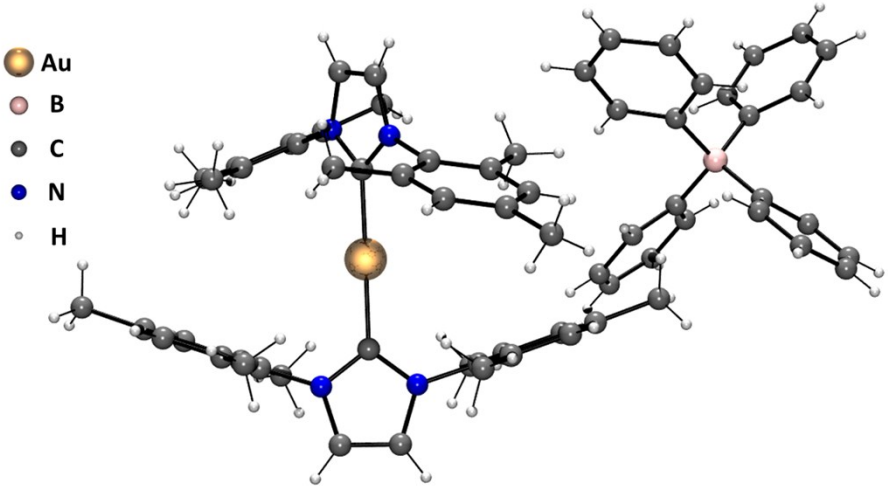

Figure 30. Crystal structure of $[Au(IMesBPh_4)_2]$ (**2c**).

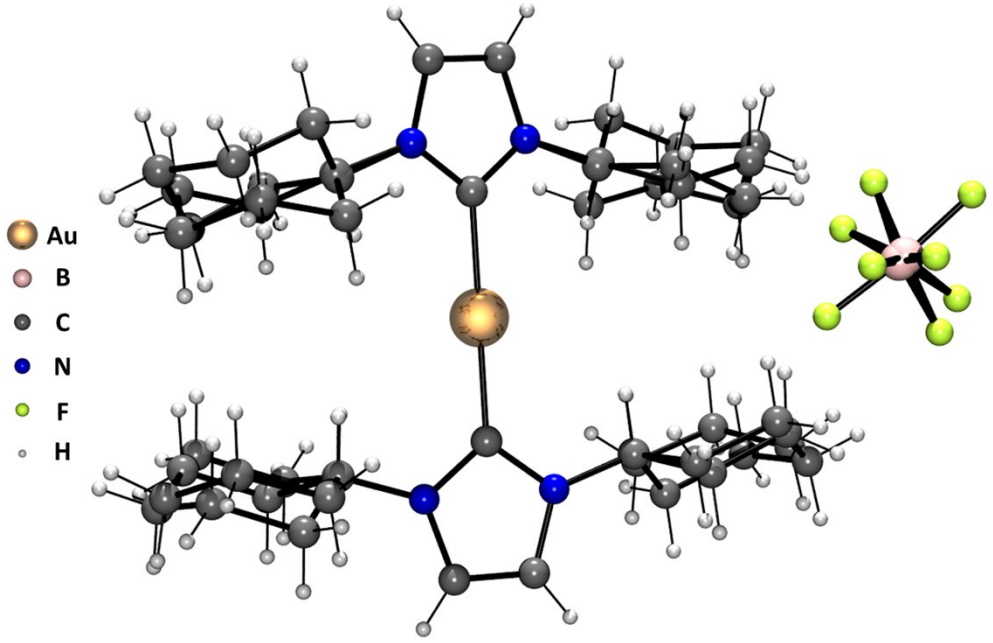

Figure 31. Crystal structure of $[Au(ICy)_2]BF_4$ (**2e**).

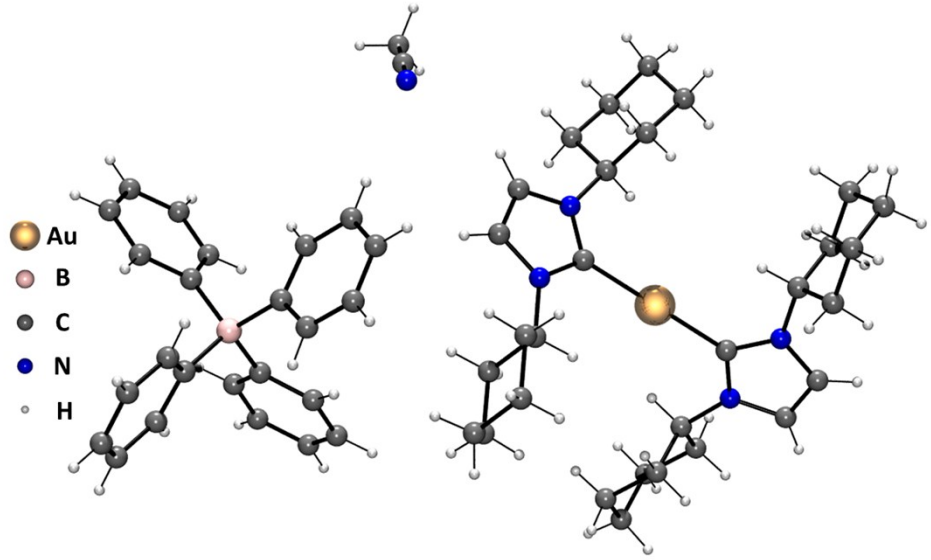

Figure 32. Crystal structure of $[Au(ICy)_2]BPh_4$ (**2f**).

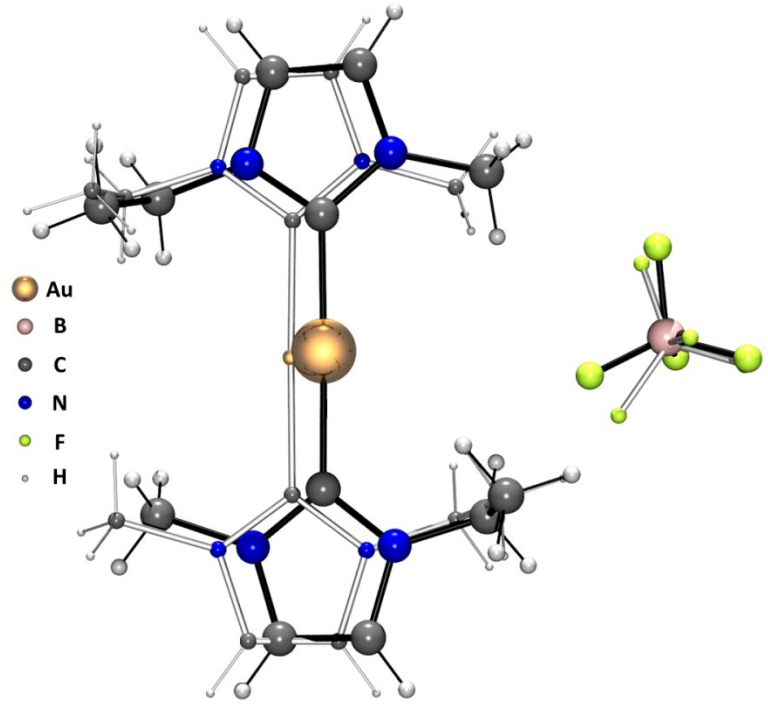

Figure 33. Crystal structure of $[Au(IEtMe)_2]BF_4$ (**2h**).

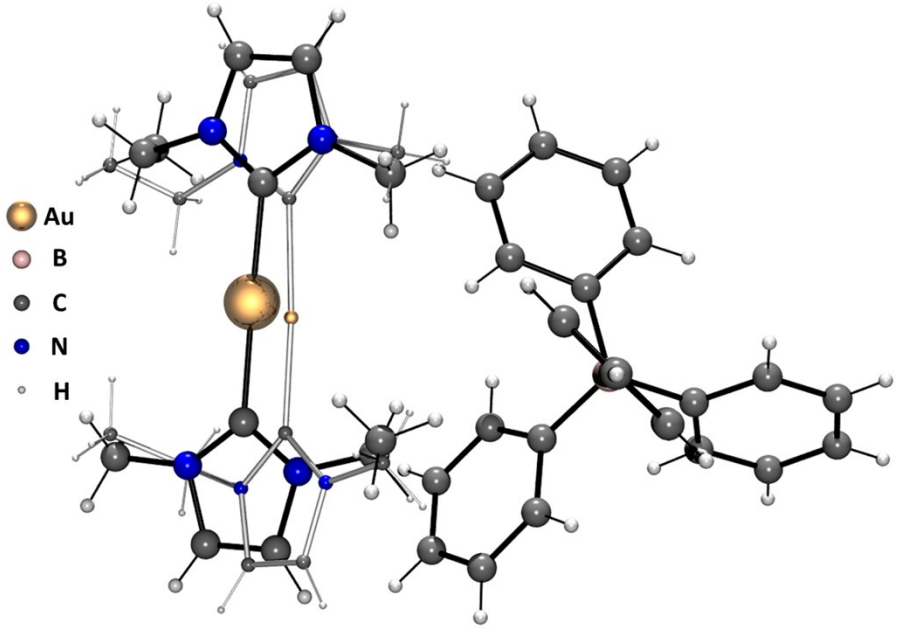

Figure 34. Crystal structure of $[Au(IEtMe)_2]BPh_4$ (**2i**).

Compound	**2a**	**2c**	**2e**	**2f**	**2h**	**2i**
Empirical formula	$C_{84}H_{96}N_8P_2F_{12}Au_2$	$C_{66}H_{68}BN_4Au$	$C_{30}H_{48}BN_4F_4Au$	$C_{58}H_{74}BN_6Au$	$C_{12}H_{20}BN_4F_4Au$	$C_{36}H_{40}BN_4Au$
Formula weight	1901.56	1125.02	748.50	1063.00	504.10	736.49
Temperature/K	293	274	294	293	293	293
Crystal system	orthorhombic	triclinic	tetragonal	monoclinic	orthorhombic	triclinic
Space group	*P*nna	*P*–1	$P4_322$	*C*2/c	*P*ccn	*P*–1
a/Å	16.44713(19)	11.79038(16)	13.93691(17)	19.8465(7)	10.9646(3)	11.566(2)
b/Å	64.8158(7)	13.8657(2)	13.93691(17)	12.1654(3)	15.1475(4)	11.987(2)
c/Å	16.02847(18)	18.2438(3)	17.2492(4)	24.9606(10)	20.6185(5)	13.298(3)
α/°	90	103.5268(12)	90	90	90	65.28(3)
β/°	90	93.6234(11)	90	115.822(5)	90	78.17(3)
γ/°	90	92.6597(11)	90	90	90	81.27(3)
Volume/Å^3	17086.9(3)	2888.25(7)	3350.44(12)	5424.8(4)	3424.45(17)	1634.6(7)
Z	8	2	4	4	8	2
ρ_{calc} g/cm^3	1.478	1.294	1.484	1.302	1.956	1.496
μ/mm^{-1}	7.329	5.097	8.638	2.753	8.630	4.530
F(000)	7616.0	1152.0	1504.0	2192.0	1920.0	736.0
Crystal size/mm^3	0.5 × 0.4 × 0.4	0.6 × 0.5 × 0.5	0.6 × 0.5 × 0.45	0.5 × 0.4 × 0.35	0.5 × 0.45 × 0.24	0.5 × 0.4 × 0.2
Radiation	CuKα (λ=1.54184)	CuKα (λ = 1.54184)	CuKα (λ = 1.54184)	MoKα (λ = 0.71073)	MoKα (λ = 0.71073)	MoKα (λ = 0.71073)
2Θ range for data collection/°	5.68 to 144.25	6.57 to 149.01	6.34 to 155.00	6.68 to 52.74	3.95 to 52.74	6.34 to 50.59
Index ranges	-20 ≤ h ≤ 18, -80 ≤ k ≤ 56, -19 ≤ l ≤ 19	-14 ≤ h ≤ 14, -17 ≤ k ≤ 17, -22 ≤ l ≤ 22	-17 ≤ h ≤ 17, -17 ≤ k ≤ 17, -21 ≤ l ≤ 14	-24 ≤ h ≤ 24, -15 ≤ k ≤ 15, -31 ≤ l ≤ 31	-13 ≤ h ≤ 13, -18 ≤ k ≤ 18, -25 ≤ l ≤ 18	-13 ≤ h ≤ 13, -14 ≤ k ≤ 14, -15 ≤ l ≤ 15
Reflections collected	90998	84484	21078	64111	10494	62940
Independent reflections	16810 [R_{int} = 0.0511, R_{sigma} = 0.0268]	11809 [R_{int} = 0.0312, R_{sigma} = 0.0155]	3541 [R_{int} = 0.0776, R_{sigma} = 0.0313]	5519 [R_{int} = 0.0623, R_{sigma} = 0.0268]	3508 [R_{int} = 0.0660, R_{sigma} = 0.0447]	5941 [R_{int} = 0.0316, R_{sigma} = 0.0160]
Data/restraints/ parameters	16810/1131/1210	11809/0/661	3541/874/315	5519/0/300	3508/1119/403	5941/242/541
Goodness-of-fit on F^2	1.276	1.067	1.146	1.073	1.070	1.029
Final R indexes [I>=2σ (I)]	R_1 = 0.0857, wR_2 = 0.1924	R_1 = 0.0253, wR_2 = 0.0689	R_1 = 0.0480, wR_2 = 0.1290	R_1 = 0.0267, wR_2 = 0.0580	R_1 = 0.0776, wR_2 = 0.2046	R_1 = 0.0263, wR_2 = 0.0567
Final R indexes	R_1 = 0.0907, wR_2 =	R_1 = 0.0263, wR_2 =	R_1 = 0.0494, wR_2 =	R_1 = 0.0308, wR_2 =	R_1 = 0.0839, wR_2 =	R_1 = 0.0408, wR_2 =

[all data]	0.1951	0.0703	0.1304	0.0595	0.2163	0.0641
Largest diff. peak/hole / e $Å^{-3}$	2.47/-3.10	0.94/-0.65	1.80/-1.63	0.45/-0.61	2.52/-3.58	0.59/-0.50

6. References

1 A. Bellido Ramos, Universite de Geneve, 2005.
2 X. Bantreil and S. P. Nolan, *Nat. Protoc.*, 2011, **6**, 69–77.
3 W. A. Herrmann, C. Köcher, L. J. Gooßen and G. R. J. Artus, *Chem. - A Eur. J.*, 1996, **2**, 1627–1636.
4 O. V. Dolomanov, L. J. Bourhis, R. J. Gildea, J. A. K. Howard and H. Puschmann, *J. Appl. Crystallogr.*, 2009, **42**, 339–341.
5 G. M. Sheldrick, *Acta Crystallogr. Sect. A Found. Crystallogr.*, 2008, **64**, 112–122.
6 WO2015/067405A1, 2015.
7 B. Liu, X. Ma, F. Wu and W. Chen, *Dalt. Trans.*, 2015, **44**, 1836–1844.
8 W. Chen, F. Liu and X. You, *J. Solid State Chem.*, 2002, **167**, 119–125.
9 M. Hans, J. Wouters, A. Demonceau and L. Delaude, *Chem. - A Eur. J.*, 2015, **21**, 10870–10877.
10 O. Stolarska, A. Soto, H. Rodríguez and M. Smiglak, *RSC Adv.*, 2015, **5**, 22178–22187.
11 F. Lazreg, D. B. Cordes, A. M. Z. Slawin and C. S. J. Cazin, *Organometallics*, 2015, **34**, 419–425.
12 M. V. Baker, P. J. Barnard, S. J. Berners-Price, S. K. Brayshaw, J. L. Hickey, B. W. Skelton and A. H. White, *Dalt. Trans.*, 2006, **6**, 3708.
13 S. Zhu, R. Liang and H. Jiang, *Tetrahedron*, 2012, **68**, 7949–7955.